

CYCLIC BEHAVIOUR OF ADAPAZARI CLAYEY SILTS

116311

**A THESIS SUBMITTED TO
THE GRADUATE SCHOOL OF NATURAL AND APPLIED SCIENCES
OF
THE MIDDLE EAST TECHNICAL UNIVERSITY**

BY

ONUR PEKCAN

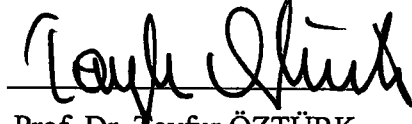
116311

**IN PARTIAL FULFILLMENT OF THE REQUIREMENTS FOR THE
DEGREE OF
MASTER OF SCIENCE
IN
THE DEPARTMENT OF CIVIL ENGINEERING**

SEPTEMBER 2001

**T.C. YÜKSEKÖĞRETİM KURULU
DOKÜMANTASYON MERKEZİ**

Approval of the Graduate School of Natural and Applied Sciences



Prof. Dr. Tayfur ÖZTÜRK

Director

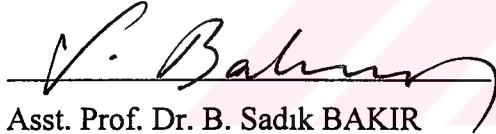
I certify that this thesis satisfies all the requirements as a thesis for the degree of Master of Science.



Prof. Dr. Mustafa TOKYAY

Head of the Department

This is to certify that we have read this thesis and that in our opinion it is fully adequate, in scope and quality, as a thesis for the degree of Master of Science.



Asst. Prof. Dr. B. Sadık BAKIR

Co-Supervisor



Asst. Prof. Dr. K. Önder ÇETİN

Supervisor

Examining Committee Members

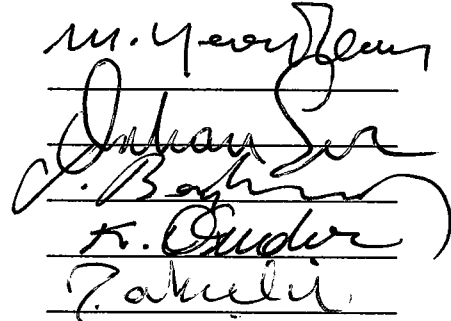
Prof. Dr. Yener ÖZKAN

Prof. Dr. Orhan EROL

Asst. Prof. Dr. B. Sadık BAKIR

Asst. Prof. Dr. K. Önder ÇETİN

Civil Eng. (M.Sc.) Nefise AKÇELİK



ABSTRACT

CYCLIC BEHAVIOUR OF ADAPAZARI CLAYEY SILTS

Pekcan, Onur

M.S., Department of Civil Engineering

Supervisor: Asst. Prof. Dr. K. Önder Çetin

Co-Supervisor: Asst. Prof. Dr. B. Sadık Bakır

September 2001, 83 pages

August 17, 1999 İzmit ($M_w=7.4$) earthquake played a key role in emphasizing the effects of local soil conditions on the damage and its distribution, which was predominant in some parts of the earthquake-affected area, more specifically the city of Adapazarı.

When the soil composition in Adapazarı is considered together with the liquefaction or cyclic softening behaviour occurred, İzmit earthquake was quite fascinating from geotechnical earthquake engineering point of view. The purpose of this study was to develop a sound understanding of the cyclic behaviour of Adapazarı clayey silt and silty clays, which forms a gap in the literature. For this purpose, series of cyclic triaxial tests were performed on five selected sites, where foundation displacements were significant. Samples were isotropically consolidated to in-situ effective stresses varying in the range of 0.45 to 0.55 atm. Volumetric strains were recorded during consolidation. Cyclic loads were chosen similar to the ones that were estimated in Adapazarı for İzmit earthquake in the range of CSR of 0.3 to 0.55 and applied with a frequency of 1 Hz. Furthermore,

the engineering properties and the particle size distribution of soil samples were determined by means of classical soil mechanics testing methods.

The cyclic triaxial tests performed on Adapazari silty clays and clayey silts were evaluated to present a clear explanation of ground failure induced damage in Adapazari. Following conclusions could be drawn from presented cyclic triaxial test results:

1. Some mixtures of silt and clay can be cyclically liquefied based on either 100% pore pressure or 5% double amplitude axial strain criteria.
2. Pore pressure build-up in silty clays and clayey silts is generally slower than that observed in sands and non-plastic silts. However, low to medium plasticity silty clays can build up significant pore pressures ($r_u > 70\%$) under reasonably low number of cyclic loads ($N < 25$) at moderate to high CSR's (~ 0.3 to 0.5).
3. Cyclic resistance of the mixtures of clays and silts increase with decrease in void ratio and increase in PI.

Keywords: cyclic soil behaviour, liquefaction, clayey silts, silts, silty clays, cyclic triaxial testing, cyclic loading, earthquake, Adapazari.

ÖZ

ADAPAZARI KİLLİ SİLTLERİNİN TEKRARLI YÜKLER ALTINDA DAVRANIŞI

Pekcan, Onur

Yüksek Lisans, İnşaat Mühendisliği Bölümü

Tez Yöneticisi: Yrd. Doç. Dr. K. Önder Çetin

Ortak Tez Yöneticisi: Yrd. Doç. Dr. B. Sadık Bakır

Eylül 2001, 83 sayfa

17 Ağustos 1999, İzmit ($M_w=7.4$) depremi, deprem bölgesinin bazı bölümlerinde ve de özellikle Adapazarı'nda meydana gelen hasar ve hasar dağılımında etkili olan yerel zemin şartlarının önemini ortaya koymakta anahtar rol oynamıştır.

Adapazarı zeminlerinin türleri, İzmit depremi sırasında Adapazarı'nda meydana gelen sıvılaşma ve dinamik yumuşama hareketleri ile beraber düşünüldüğünde, geoteknik deprem mühendisliği açısından oldukça ilginç bir durum oluşturmaktadır. Bu çalışmanın amacı, literatürde bir boşluk oluşturan ve Adapazarı'nda sıkça bulunan killi silt ve siltli killi zeminlerin dinamik davranışını açıklamaktır. Bu amaçla, önemli temel deplasmanları görülen beş alandan alınan numuneler üzerinde dinamik üç eksenli deneyler uygulanmıştır. Numuneler izotropik olarak, 0.45 ile 0.55 atmosfer arası olarak tahmin edilen saha yükleri

altında konsolide edilmiştir. Konsolidasyon sırasında hacimsel deformasyonlar kaydedilmiştir. Dinamik yükler İzmit depreminde Adapazarı'nda meydana gelen yüklere benzer şekilde (Tekrarlı Gerilme Oranı, 0.3 ile 0.55 arası) seçilmiş ve 1 Hz. frekans ile uygulanmıştır. Ayrıca numunelerinin mühendislik parametreleri ve gradasyon özellikleri klasik zemin mekaniği deneyleri kullanılarak bulunmuştur.

Adapazarı silti killeri ve killi siltleri üzerinde yapılan dinamik üç eksenli deneyler, meydana gelen temel deplasmanlarının açıklanması amacıyla yorumlanmıştır. Çıkan sonuçlar aşağıdaki gibi özetlenebilir:

1. Bazı silt ve kil karışımları tekrarlı yükler altında 100% boşluk suyu basıncı oluşması veya %5 iki yönlü eksenel deformasyon kriterlerine göre sıvılaşabilirler.

2. Siltli killer ve killi siltlerde boşluk suyu basıncı oluşumu kumlarda ve plastik olmayan siltlerdeki göre daha yavaştır. Ancak, düşük ve orta plastisiteli siltli killerde oldukça düşük tekrarlı yük sayılarında ($N < 25$) ve ortadan yükseğe değişen tekrarlı gerilme oranlarında (~ 0.3 ile 0.5) önemli boşluk suyu basıncı oluşumları ($r_u > 70\%$) gözlenmiştir.

3. Kil ve silt karışımlarının dinamik dayanımları boşluk oranında ki azalma ve platisite değerindeki artışla beraber artmaktadır.

Anahtar Kelimeler: tekrarlı yüklerde zemin davranışı, sıvılaşma, killi siltler, siltler, siltli killer, dinamik üç eksenli test metodu, tekrarlı yükleme, deprem, Adapazarı.

to the memory of those who lost their lives during the İzmit and Düzce earthquakes

ACKNOWLEDGEMENTS

I would like to thank to my supervisor Assistant Prof. Dr. K. Önder Çetin, first for sharing his great scientific enthusiasm with me, which enabled the continuity of the study and for helping me in performing the dynamic soil testings. His reviewing of the thesis many times to have the quality, which a scientist always looks for, is worth mentioning here. Finally, it should not be forgotten that the courage necessary to start this study belongs to him.

My co-supervisor Assistant Prof. Dr. Sadık Bakır is greatly thanked for his careful review of my thesis and scientific approach during my study. His positive attitude and patience throughout this study made me feel comfortable. Furthermore, his efforts for sponsoring me is worth to remember.

My thanks and sincere appreciations go to the soil mechanics laboratory technician Mr. Ali Bal for helping me to master the art of soil testing during this study. His contributions were invaluable and more importantly, his teachings in ethics and humanity for me were immense.

I thank to Associated Prof. Dr. Uğur Polat, Prof. Dr. Mustafa Tokyay and General Directorate of Highways, especially to the director of Soil Mechanics and Tunnelling Division, Mrs. Nefise Akçelik, for their contributions, which made the operation of the cyclic triaxial testing machine possible.

My roommate Mahmut Yavuz Şengör is acknowledged for his friendship, patience, understanding and great help during this study.

My dear friends Engin Yılmaz, İsmail Çağrı Özcan, Nejan Huvaj, Özlem Özmütlu, Özlem Şaşal and Ebru Özel are also acknowledged for their moral support throughout the study. Their presence makes me happy.

Special thanks go to my school friends Ayşegül Askan, Ali Cihan Pay, and Serhat Bayılı for their friendship and help.

I thank Ms. Meltem Güvener and especially her valuable friend for helping me to think about the nature of life, to make right decisions in my life and to smile like just they did when I was having difficulties although they were not aware of what their contributions to me were.

In the name of Engin Karaesmen, Bengi Öner and Gülçin Özmen, I express my sincere gratitude to all my teachers who have brought me today by sharing their experiences throughout my education.

My heartfelt thanks go to all my aunts, mother's brother and cousins, especially to Mrs. Aynur Özçelik, for their patience and understanding during the study.

My sincere thanks go to Mr. İzzet Özdemir for all his contributions!

The last but the most I am grateful to my mother, Neslihan Pekcan, that I owe my all. There is nothing to say, Just Love!

TABLE OF CONTENTS

ABSTRACT	iii
ÖZ	v
DEDICATION	vii
ACKNOWLEDGEMENTS	viii
TABLE OF CONTENTS	x
LIST OF TABLES	xiii
LIST OF FIGURES	xiv
Chapter 1 INTRODUCTION	
1.1 Research Statement	1
1.2 Liquefaction Definition	2
1.3 Problem Significance and Limitations of Previous Studies	3
1.4 Scope and Organization	5
Chapter 2 AN OVERVIEW OF THE CITY OF ADAPAZARI	
2.1 Introduction	6
2.2 Seismicity of Adapazar	6
2.3 The General Characteristics of zmit Earthquake	7
2.4 An Overview of Adapazar Geology	9
2.5 Subsurface Characteristics of Adapazar	11
2.6 Observed Foundation Deformations	13

Chapter 3 CYCLIC TRIAXIAL TESTING

3.1 Introduction	18
3.2 Cyclic Triaxial Testing	18
3.3 Mechanics of Cyclic Triaxial Testing	19
3.3.1 Idealised Field Loading Conditions	19
3.3.2 Mechanics of Cyclic Triaxial Testing	19
3.4 Advantages and Limitations of Cyclic Triaxial Testing	24
3.5 Norwegian Cyclic Triaxial Apparatus	25
3.5.1 Cyclic Triaxial System Components	26
3.5.1.1 Triaxial Cell	26
3.5.1.2 Loading System Components	27
3.5.1.3 Transducers and Signal Conditioner	27
3.5.1.4 Process Interface Unit	28
3.5.1.5 Computer	28
3.6 General Testing Procedure	28
3.6.1 Sample Preparation	29
3.6.1.1 Trimming the Sample	29
3.6.1.2 Placing the Filter Paper	29
3.6.1.3 Placing the Sample	30
3.6.2 Sample Consolidation	31
3.6.2.1 Developing the Desired Cell Pressure	31
3.6.2.2 Consolidation of the Specimen	32
3.6.3 Sample Saturation	32
3.6.4 Calibration	34
3.6.5 Cyclic Testing	35
3.6.5.1 Assembling the Force Transducer and the Displacement Gage	35
3.6.5.2 Starting the Test	37

3.6.5.3 During the Test	37
3.6.5.4 Unloading and Stopping the Test	38
3.6.5.5 Removing the Sample	38
3.7 Laboratory Data Correction	39
3.7.1 Incorrect Planes of Failure	39
3.7.2 Bi-direction Loading Effects	40
Chapter 4 INTERPRETATION OF RESULTS	
4.1 Introduction	41
4.2 Cyclic Triaxial Test Results	41
4.2.1 Definitions of Terms Used in 4-way Graphs	42
4.2.2 Site C	44
4.2.3 Site D	50
4.2.4 Site E	55
4.2.5 Site G	60
4.2.6 Site J	66
Chapter 5 SUMMARY AND CONCLUSION	
5.1 Summary	74
5.2 Conclusion	76
5.4 Recommendations for Future Study	79
REFERENCES	80

LIST OF TABLES

TABLE

1-1	Liquefaction Susceptibility of Silty and Clayey Sands	4
2-1	Physical Characteristics of İzmit Earthquake	8
2-2	Field Log Details Of The Samples	17
3-1	Recommended C_r Values For Various Field Conditions	39
4-1	Engineering Properties of Specimen C1-1	45
4-2	Engineering Properties of Specimen C1-3	47
4-3	Engineering Properties of Specimen D2-1	51
4-4	Engineering Properties of Specimen D2-2	53
4-5	Engineering Properties of Specimen E1-2	56
4-6	Engineering Properties of Specimen E1-3	58
4-7	Engineering Properties of Specimen G2-1	61
4-8	Engineering Properties of Specimen G2-5	63
4-9	Engineering Properties of Specimen J3-1	67
4-10	Engineering Properties of Specimen J3-2	69
4-11	Engineering Properties of Specimen J3-3	71
5-1	Summary of the engineering properties and CSR_x values for all specimens	75

LIST OF FIGURES

FIGURE	
2.1	Historical Overview of NAF Zone 7
2.2	The East-West Component of İzmit Earthquake 8
2.3	General Overview of Adapazarı Surface Geology 10
2.4	The Location Of The Sites On Adapazarı Map 14
2.5	Overview of Site C (40.78370° N, 30.39221° E) 15
2.6	Overview of Site D (40.76929° N, 30.40828° E) 15
2.7	Overview of Site E (40.77778° N, 30.40518° E) 16
2.8	Overview of Site G (40.77450° N, 30.40896° E) 16
2.9	Overview of Site J (40.77518° N, 30.41077° E) 16
3.1	Illustration of Earthquake Induced Stresses on a Soil Element ... 20
3.2	Simulation of Cyclic Shear Stress on a Plane for a Triaxial Test Specimen 21
3.3	Simulation of Cyclic Triaxial Testing 23
3.4	Norwegian Cyclic Triaxial Machine 26
3.5	TLT Interface 34
3.6	Calibration Interface of TLT 36
4.1	Particle Size Distribution for Specimen C1-1 45
4.2	CTX Results for Specimen C1-1 46
4.3	Particle Size Distribution for Specimen C1-3 47
4.4	CTX Results for Specimen C1-3 48

4.5 CSR vs. Number of Cycles for Site C	49
4.6 Particle Size Distribution for Specimen D2-1	51
4.7 CTX Results for Specimen D2-1	52
4.8 Particle Size Distribution for Specimen D2-2	53
4.9 CTX Results for Specimen D2-2	54
4.10 CSR vs. Number of Cycles for Site D	55
4.11 Particle Size Distribution for Specimen E1-2	56
4.12 CTX Results for Specimen E1-2	57
4.13 Particle Size Distribution for Specimen E1-3	58
4.14 CTX Results for Specimen E1-3	59
4.15 CSR vs. Number of cycles for Site E	60
4.16 Particle Size Distribution for Specimen G2-1	61
4.17 CTX Results for Specimen G2-1	62
4.18 Particle Size Distribution for Specimen G2-5	63
4.19 CTX Results for Specimen G2-5	64
4.20 CSR vs. Number of Cycles for Site G	66
4.21 Particle Size Distribution for Specimen J3-1	67
4.22 CTX Results for Specimen J3-1	68
4.23 Particle Size Distribution for Specimen J3-2	69
4.24 CTX Results for Specimen J3-2	70
4.25 Particle Size Distribution for Specimen J3-3	71
4.26 CTX Results for Specimen J3-3	72
4.27 CSR vs. Number of Cycles for Site J	73
5.1 Liquefaction Susceptibility of Silty and Clayey Sands and the findings of this study	77
5.2 CSR _{in-situ} vs. Number of cycles for 3% Shear Strain	78
5.3 CSR _{in-situ} vs. Number of cycles for 7.5% Shear Strain	78

CHAPTER 1

INTRODUCTION

1.1 RESEARCH STATEMENT

In 1999, Turkey was shaken by two major earthquakes: August 17, İzmit ($M_w=7.4$) and November 12, Düzce ($M_w=7.1$) earthquakes, both along the North Anatolian fault. Although these earthquakes affected the northwestern part of Turkey severely, İzmit earthquake was different than Düzce earthquake in the sense that the effects of local soil conditions on the damage and its distribution was predominant in some part of the earthquake-affected area, more specifically the city of Adapazarı.

After İzmit earthquake, it was observed that the foundation failure patterns as a result of cyclic liquefaction and mobility of foundation soils were different than the ones observed after the big earthquakes occurred in the past, such as, 1964 Niigata ($M_w=7.5$), 1971 San Fernando ($M_w=6.6$), 1994, Northridge ($M_w=6.8$) or 1995, Hyogo-Ken Nanbu ($M_w=6.9$) earthquakes. Especially in Adapazarı, located over young riverbed sediments with soft and liquefiable clayey silts and sands, hundreds of buildings settled as much as 1.5 m, or tilted due to liquefaction-induced softening and shear strength loss of the foundation soils. Punching of buildings into cyclically softened foundation soils caused occasional bulging of sidewalk's, suggesting constant volume behaviour. Surface manifestations of liquefaction in Adapazarı including sand boils and a few lateral-spreads were ample. Additionally, horizontal translations of buildings were observed presenting interesting case histories (Erdik, 2001).

The main goal of this study presented here is to develop a clear understanding of cyclic behaviour of Adapazari silty clayey soils, which contributed to the observed foundation displacements. For this purpose, series of isotropically consolidated undrained cyclic triaxial tests ($\overline{\text{ICU-TX}}$) were performed on samples obtained from Adapazari foundation failure sites. As a result of the findings from $\overline{\text{ICU-TX}}$ tests, observed foundation displacements ranging from a couple of centimeters to well over a meter contributing to the observed devastating damage in Adapazari could be clearly predicted and their mechanisms can be understood.

1.2 LIQUEFACTION DEFINITION

The phenomena of soil liquefaction has been recognized for many years. Terzaghi and Peck (1948) addressed the “spontaneous liquefaction” issue to describe the significant loss of strength of very loose sands causing flow failures due to slight disturbance. Mogami and Kubo (1953) also used the same term to define shear strength loss due to seismically-induced cyclic loading.

“It was not until the Alaska and Niigata earthquakes that geotechnical engineers took serious interest in the general phenomenon of earthquake-induced liquefaction or the conditions responsible for causing it to occur in the field” (Seed and Lee, 1976).

Following the 1964 Niigata earthquake, many Japanese researchers (Kishida (1966), Koizumi (1966), Ohsaki (1966)) studied characterization of the behavior of liquefied and non-liquefied soil layers based primarily on Standard Penetration Test (SPT) results. Parallel to these, laboratory-based efforts continued to provide new insight into the undrained behavior of “loose” and “dense” sands under cyclic loading (Seed and Lee, 1966).

In the literature, the term liquefaction has been used to define flow failures and cyclic softening (cyclic liquefaction and cyclic mobility behaviors) which represent fundamentally different soil responses. Flow liquefaction applies to strain softening soils in undrained loading and requires in-situ shear stresses to be greater than the ultimate or minimum undrained shear strength. Cyclic softening behavior can be observed in both strain softening and strain hardening materials. Cyclic softening response can take two different forms: (1) Cyclic liquefaction : requires shear stress reversals (instantaneous zero shear strength) during undrained loading, and (2) Cyclic mobility : requires shear stresses during undrained loading to be always greater than zero. More detailed discussions of flow failure and cyclic softening mechanisms are presented in Seed (1976), Castro and Poulos (1976), National Research Council (1985), and Robertson and Fear (1997).

In most cases, limitations in the extent of available data from actual liquefaction and nonliquefaction case histories don't enable researchers to actually pursue the identification of different liquefaction-induced failure mechanisms. Within the scope of this study, "liquefaction" is identified by observable surface manifestations such as sand boils, ground cracking, lateral spreading, settlements and bearing capacity failures. Thus the in-situ evidence of "liquefaction" takes a variety of very different forms, some far more catastrophic than others.

1.3 PROBLEM SIGNIFICANCE AND LIMITATIONS OF PREVIOUS STUDIES

Liquefaction of cohesionless soils is known as a major cause of damage in earthquakes (e.g. the 1964 Alaska and Niigata, 1983 Nihonakai-Chubu, 1987 Elmore Ranch and Superstition Hills, 1989 Loma Prieta, 1993 Kushiro-Oki, 1994 Northridge, 1995 Hyogoken Nanbu - Kobe, 1999 İzmit earthquakes). Researchers have spent significant efforts on simulating cyclic behaviour of cohesionless soils with limited plastic and non-plastic fines (Seed and Lee, 1966; Vucetic and

Dobry, 1991; Boulanger and Seed, 1995; Polito and Martin, 2001). Still, very little is known regarding the cyclic behaviour of clayey silt and sandy silt mixtures of medium to high plasticity.

As shown in Table 1-1, clayey silts with clay content and liquid limit higher than 10 % and 32 % respectively are commonly defined as not susceptible to liquefaction. However it has been clearly shown by evidences obtained after 1999 İzmit earthquake that these soils can actually liquefy. This study clearly showed that significant pore pressure and strain could be developed as a result of cyclic loading of clayey silt and silty clay samples.

Table 1-1 Liquefaction Susceptibility of Silty and Clayey Sands (after Andrews and Martin, 2000)

	Liquid Limit ¹ < 32	Liquid Limit ≥ 32
Clay Content ² < 10%	Susceptible	Further Studies Required <i>(Considering plastic non-clay sized grains – such as Mica)</i>
Clay Content ² ≥ 10%	Further Studies Required <i>(Considering non-plastic clay sized grains – such as mine and quarry tailings)</i>	Not Susceptible

Notes:

1. Liquid limit determined by Casagrande-type percussion apparatus.
2. Clay defined as grains finer than 0.002 mm.

1.3 SCOPE AND ORGANIZATION

Following this chapter of introduction, Chapter 2 presents an overview of the city of Adapazarı including brief summaries of seismicity and geologic setting as well as the characteristics of İzmit Earthquake.

Chapter 3 discusses the implemented cyclic triaxial testing program. Brief definitions of testing apparatus including the developed data acquisition component as well as the procedures followed during different phases of the cyclic are also presented.

The results of cyclic triaxial tests are presented in Chapter 4. Brief discussions of the test results are also included in each section.

Finally, a summary of the research, major conclusions, and recommendations for future areas of study are presented in Chapter 5.

CHAPTER 2

AN OVERVIEW OF THE CITY OF ADAPAZARI

2.1 INTRODUCTION

As the central district of Sakarya province, Adapazarı, with a population of over 180,000 people is an important city, home to rapidly developing industry. The city is densely developed within the last decade primarily with 3 to 5 story reinforced concrete buildings. These buildings are characterized as non-ductile structures. Due to shallow ground water table depths (~0.5 to 1.0m) as well as relatively low bearing capacities of underlying soils, the foundations were designed as reinforced concrete shallow mat foundations usually located at water table depths.

2.2 SEISMICITY OF ADAPAZARI

Adapazarı, located within about 4 km of the most prominent active fault in Turkey, North Anatolian Fault (NAF), has been shaken by numerous large earthquakes throughout the history. As shown in Figure 2.1, previous to the earthquakes of 1999, 7 big earthquakes on the NAF, loading the segments between Düzce and Çınarcık which later ruptured causing the earthquakes of İzmit and Düzce.

A relatively well-documented past earthquake in Adapazarı was the one on July 10, 1894 which caused 60 deaths and significant damage over 3,000 of total 4,000 houses. Similarly, the June 20, 1943 earthquake caused extensive

damage leading to 300 casualties. A relatively recent earthquake affecting Adapazarı is the one on Mudurnu Fault System, July 22, 1967, the Mudurnu Valley earthquake of $M_w=7.1$. The reported damage in Adapazarı was significant and evidence of liquefaction in the form of sand boils and lateral spreads were observed (Ambraseys and Zapotek, 1969)

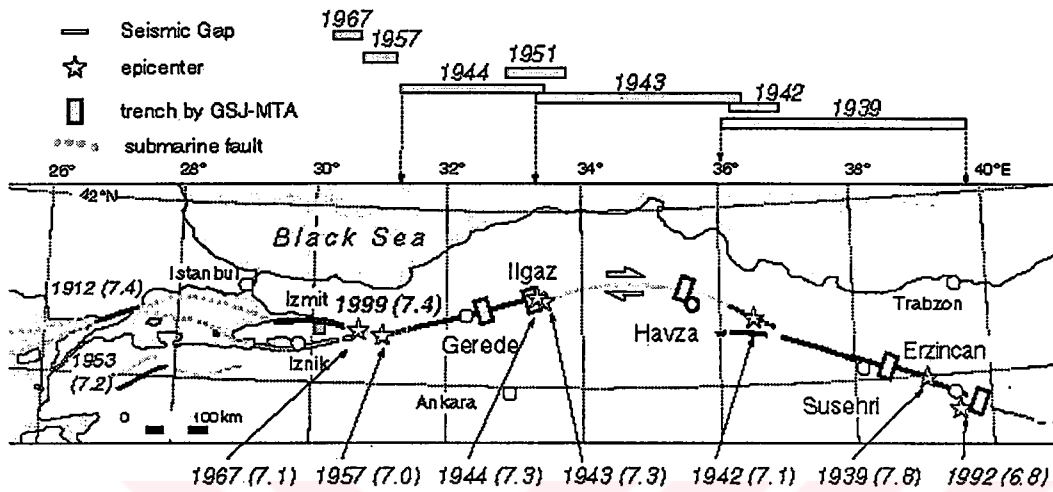


Figure 2.1 Historical Overview of NAF Zone

2.3 THE GENERAL CHARACTERISTICS OF İZMİT EARTHQUAKE

In August 17, 1999, an earthquake of magnitude $M_w = 7.4$ occurred on the North Anatolian Fault Zone. The macroseismic epicenter was near the town of Gölcük in the western part of Turkey. The earthquake record provided by Sakarya ground motion station only in the east-west direction is shown on Figure 2.2 since the north-south component of the station malfunctioned.

The station recorded a peak horizontal ground acceleration, velocity and displacement of 0.399g, 79.80 cm/s and 198.64 cm, respectively, and was classified as a rock site (Rathje, 2001). The station is located in the southwestern

corner of Adapazarı and at a distance 3.3 km from the fault rupture surface. Most of the aftershock activity is confined to the region bounded by 40.5-40.8N and

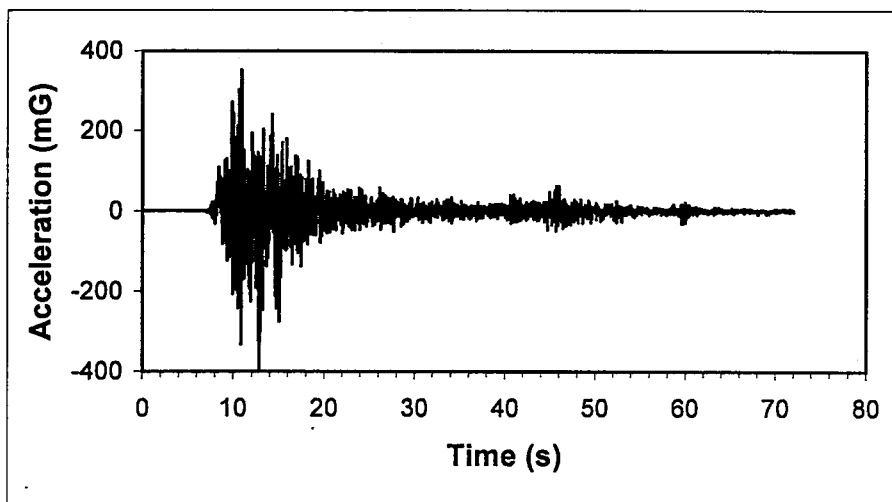


Figure 2.2 The East-West Component of İzmit Earthquake

29.8-30.0E, which covers the area between İzmit and Adapazarı to the east of the epicentre. Main-shock ground motions recorded at similar site-source distances suggest that the peak horizontal ground acceleration in Adapazarı be on the order of 0.3 to 0.5g. Additionally, three significant aftershocks followed the main shock within an hour and produced peak accelerations of 0.16g, 0.10g and 0.15g at the Sakarya strong motion station (Earthquake Spectra, Chapter 8, 2000). The physical characteristics of İzmit earthquake are outlined in Table 2-1.

Table 2-1 Physical Characteristics of İzmit Earthquake

Date and time	1999-08-17 at 00:01:39.80 (utc), 03:01:37 a.m. local time
Surface wave magnitude	7.8 (usgs)
Body wave magnitude	6.3 (usgs)
Duration magnitude	6.7 (kandilli)
Moment magnitude	7.4 (usgs, kandilli)
Epicenter	40.702n, 29.987e (usgs)
Epicentral Depth	17 km. (usgs)

2.4 AN OVERVIEW OF ADAPAZARI GEOLOGY

In general, most of the city, including the downtown area, lies within a sedimentary basin. In fact, the word “adapazari” in Turkish means, “island market”. The city is so named because it occupies a landmass between two meandering rivers on an old east-west trade route. Pleistocene and Holocene alluvial deposits overlie older lakebed sediments, with the most recent Holocene materials deposited over much of the city by the Sakarya River and its tributaries. The Sakarya River originally flowed westward through Lake Sapanca into the Marmara Sea, now flows northward through the Adapazari basin to the Black Sea. As evidence of the active fluvial processes in the Adapazari Basin, a masonry bridge built in 559 A.D. on the old alignment of the Sakarya River is now 4 km west of the current river (Ambraseys and Zatopek, 1969). As shown in Figure 2.3, the surficial geology of Adapazari consists generally of young alluvium but transitions into Upper Cretaceous flysch in hills at the southwestern part of the city. (Earthquake Spectra, Chapter 8, 2000)

The city and its surroundings have the units consisting of three different geologic settings: the rock formation, transition zone and alluvium from engineering properties point of view. The rock formation is mainly the accumulation of cemented dense minerals and grains. The formations of these minerals or grains are such that they are very strongly bound and resistant to water. This rock formation, which surrounds the Sakarya River basin from north and west, forms generally mid-height hills allowing a high topography and is consisting of rocks having different age and compositions. The cretaceous bedrock consists primarily of marls, sandstones, conglomerates and limestone.

The second unit, i.e. the transition formation, is mainly the intermediate formation having relatively less strongly bound, but much stiffer compared to alluvium. The alluvial layers encompass the grains having uncemented or

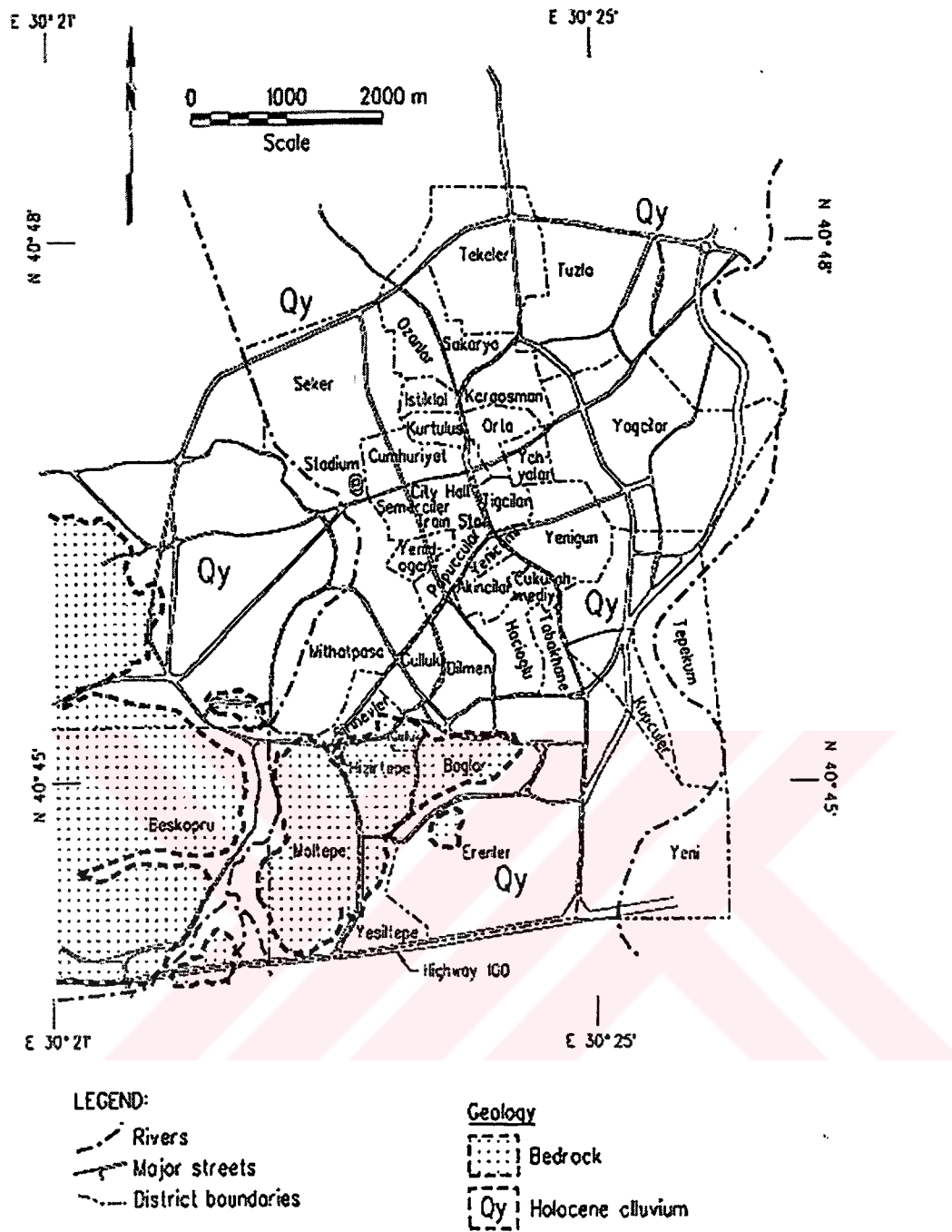


Figure 2.3 General Overview of Adapazarı Surface Geology

weakly cemented particles, which can be classified as mixtures of gravel, sand, silt and clays of Quaternary age. These are the deposits that settled mainly from Sakarya River, Mudurnu and Çark Creeks in Sakarya Basin, which cover almost 95% of the central district in the basin. Furthermore, there are organic clays and clays which are swamp deposits and grey, green or black in colour. Other than these formations, there is one more unit called alteration zone, which generally overlies the rock formation and having more resistance when compared to alluvium layer, being composed of minerals and small rock grains.

2.5 SUBSURFACE CHARACTERISTICS OF ADAPAZARI

The subsurface conditions at Adapazari are such that large variations of soil types and properties are to be expected in both, vertical and horizontal directions due to active sedimentation and fluvial action. The heterogeneity of the deposits is evidenced by a series of layers of clayey, sandy and gravelly soils. Microtremor studies performed (Tezcan, 1973) suggest that the fundamental period of much of the alluvium in Adapazari is approximately 0.3 to 0.5 seconds. However, seismic site response analyses, of typical soil columns in Adapazari (Yarar et al., 1977) indicate fundamental periods of the deep soil deposits of approximately 1.25 to 1.5 seconds.

When the boring logs obtained from the centrum are compiled and interpreted, it is seen that thickness of the Quaternary fill exceeds 120 m. In the first 30 meters of the fill, there are silt, silty sand, fine sand, silty clayey sand, silty sandy clay, and silty clayey sand formations. These flooding plain deposits reach to the maximum thickness where the urbanization and population become dense. Although subject to seasonal changes, the depth of ground water in the basin is generally only 1 to 2 m (17 Ağustos 1999 Gölcük- Arifiye -Kuzeydoğu Marmara- Depremleri Sonrası Sakarya İli ve Ona Bağlı Yerleşkeler İçin Yerleşim Alanları Araştırma Raporu, 1999).

A series of borings performed in Adapazarı indicates the following profiles:

Profile 1 (Güllük District):

- 0-2.5 m. : Silty Clay
- 2.5-5 m. : Sand and Silt (groundwater at 0.5 m.)
- 5-7.5 m. : Silt
- 7.5-10 m. : Clayey Silt (end of boring)

Profile 2 (Mithatpaşa District):

- 0-0.5 m. : Artificial Fill
- 0.5-3.5 m. : Clayey Silt (groundwater at 1.5 m.)
- 3.5-10 m. : Silty Sand
- 10-12.5 m. : Sand (end of boring)

Profile 3 (Yenidoğan District):

- 0-0.5 m. : Artificial Fill
- 0.5-4 m. : Sand and Silt (groundwater at 0.5 m.)
- 4-8.5 m. : Sand and Silt
- 8.5-12.5 m. : Sand (end of boring)

Another boring, which is located in a heavily damaged industrial part of Adapazarı, indicates poorly graded sand with N values as low as 8 underlying the surficial clay layer. The underlying dense gravelly sand had higher blow-counts, exhibiting N values above 40. This borehole reached a depth of 10 m. A “typical” soil profile consists of the following:

0-3 m.	: Silty sand (N=7); groundwater at 2 m.
3-9 m.	: Low plasticity silt with sand seams (N=5-8)
9-14 m.	: Silty sand (N=10-22)
14-22 m.	: Clayey soil (end of boring)

The “average” soil profile developed by Yasar et al. (1977) shows the groundwater at a depth of 1.8 m, with alternating layers of silty sand and silty clay extending to a depth of 75 m followed by a clay layer from 75 m to 150 m and a gravel layer that extends from a depth of 150 m to 200 m where bedrock is encountered. The estimated shear wave velocities of the soil column range from 200 m/s near the surface to about 300 m/s over the upper 34 m., followed by higher velocities increasing from 400 m/s to 700 m/s in the lower soils, with the bedrock shear wave velocity estimated as 1000 m/s. According to the information compiled on subsurface characteristics, the depth of the bedrock varies from 75 m to 200 m across the central part of Adapazari.

2.6 OBSERVED FOUNDATION DEFORMATIONS

The investigations performed immediately after the August 17, 1999 İzmit earthquake revealed that most of the damage was concentrated on 3 to 5 story buildings with inadequate shear capacity. The foundation ground deformations ranged from a couple of centimeters to over 1 m settlements and similarly from a couple of centimeters to 30 cm lateral offsets. For some marginal cases these lateral movements reached to a meter.

Twelve sites were carefully selected covering a wide range of foundation soils and foundation displacements as shown in Figure 2.4. In Figures 2.5 through 2.10 some of the observed damage at these sites are presented. Subsurface characterization studies performed, include standard penetration test (SPT), cone penetration test (CPT), seismic cone penetration test (SCPT), as well as shear wave velocity (V_s) measurements.

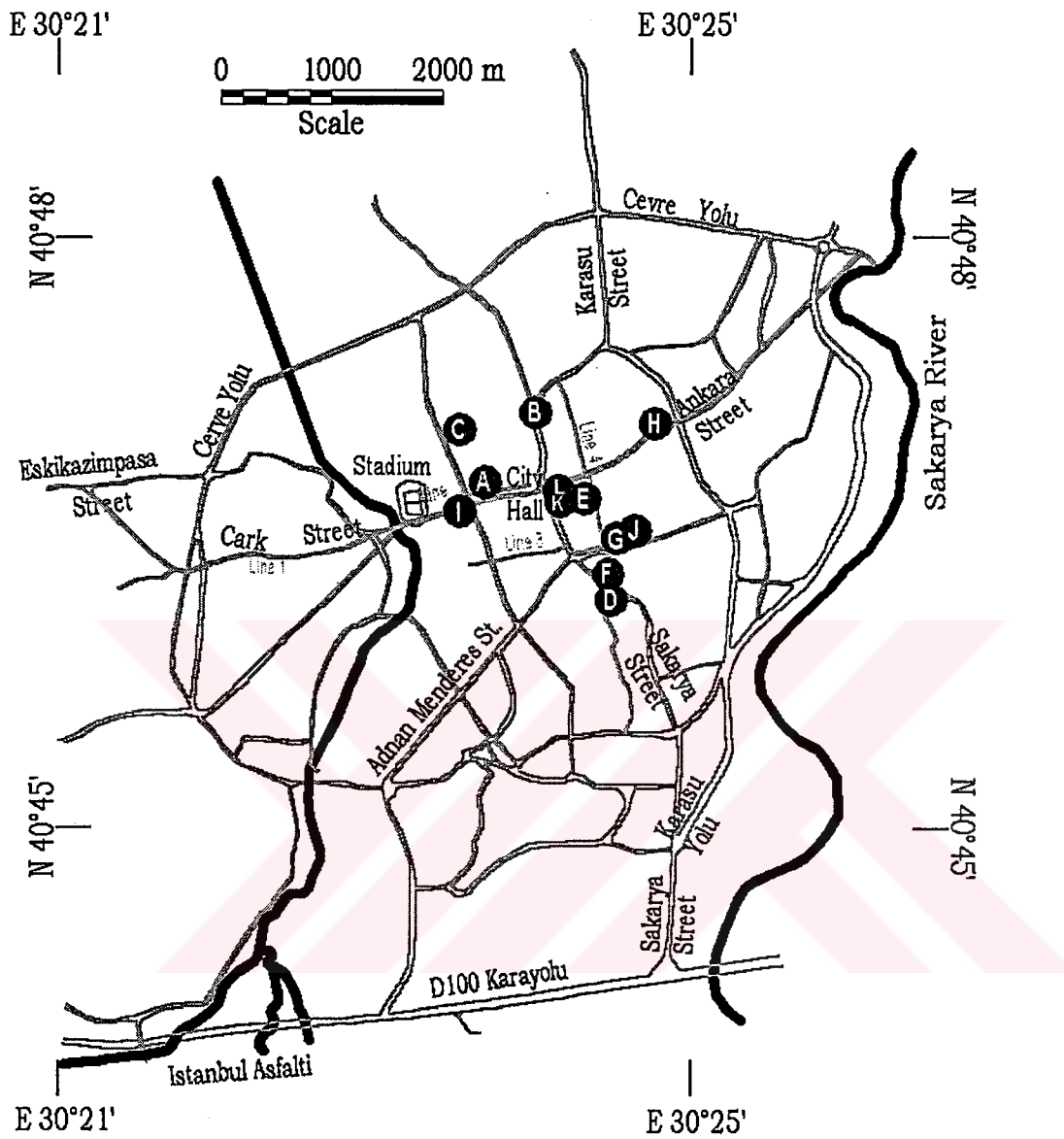


Figure 2.4 The Locations of the Sites in Adapazarı

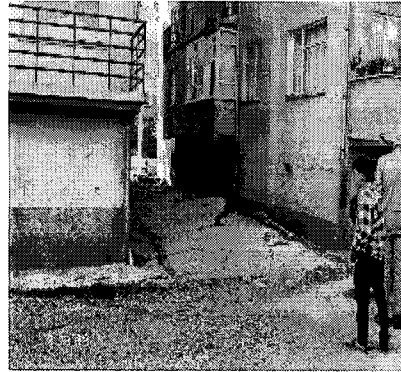


Figure 2.5 Overview of Site C (40.78370° N, 30.39221°E)

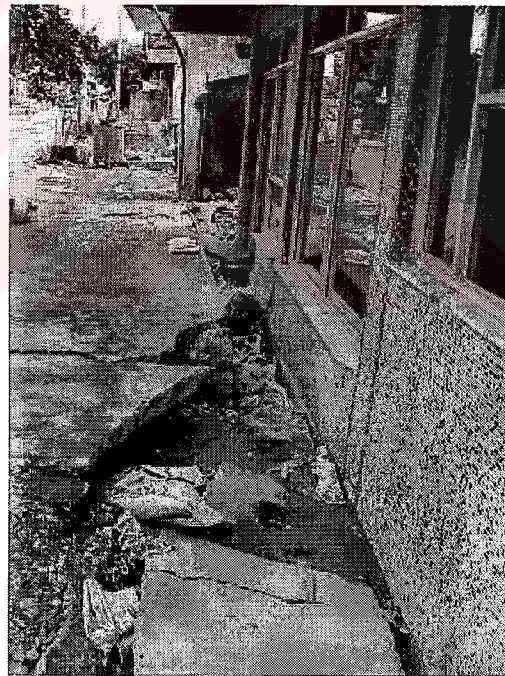


Figure 2.6 Overview of Site D (40.76929° N, 30.40828°E)

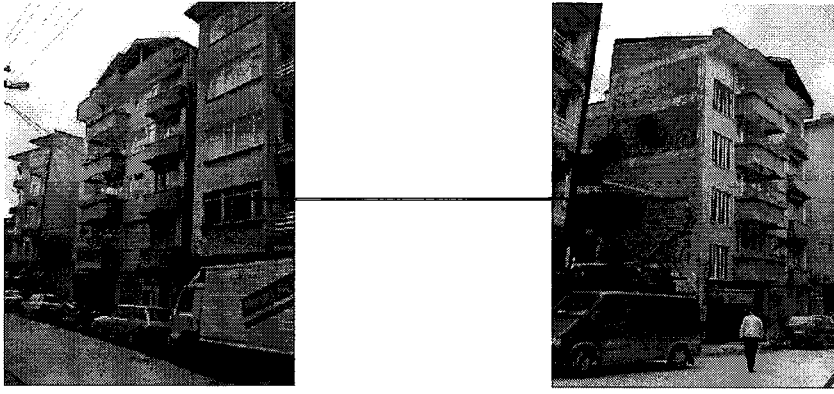


Figure 2.7 Overview of Site E (40.77778° N, 30.40518° E)



Figure 2.8 Overview of Site G (40.77450° N, 30.40896° E)



Figure 2.9 Overview of Site J (40.77518° N, 30.41077° E)

As the details are provided in Table 2-2, five undisturbed samples from different sites were acquired using thin wall Shelby tubes for the purpose of cyclic triaxial testing.

Table 2-2 Field Log Details of The Samples

Borehole ID	Sample ID	Depth (m)	Length of Sample (m)	Soil Description Based on Field Logs	Depth to Water Table (m)
SPT-C1	C1-3/ UD-1	3.40	40	Brown Clayey Silt	1.4
SPT-D2	D2-1/ UD-1	1.30	42	Gray Clayey Silt	1.4
SPT-E1	E1-4/ UD-1	4.50	35	Gray Silty Clay	0.7
SPT-G2	G2-3/ UD-1	3.30	80	Top: Silty Fine Sand Bottom: Gray Clayey Silt	0.4
SPT-J3	J3-1/ UD-1	2.30	38	Top: Clayey Silt with Fine Sand Bottom: Gray Silt with Fine Sand	1.7

CHAPTER 3

CYCLIC TRIAXIAL TESTING

3.1 INTRODUCTION

Since the extensive foundation displacements of various forms observed in Adapazarı during İzmit earthquake is predominantly governed by the cyclic response of underlying clayey silts and silty clays, understanding their behaviour will establish a big step towards explaining the consequences. Therefore, an intensive cyclic laboratory-testing program was to be implemented. This chapter discusses the adopted cyclic triaxial testing program for the Adapazarı soils.

3.2 CYCLIC TRIAXIAL TESTING

The behaviour of soils is quite different under cyclic loading when compared to static loading. Therefore, it is natural to expect the use of differently characterized and equipped tests, compared to those used in static loading to simulate and understand the dynamic behaviour of the soils. Despite this fact, the cyclic triaxial testing methodology is actually the adaptation of static triaxial testing to dynamic conditions by introducing a cyclic load. Seed and Lee (1966) were the first to publish the methodology in the literature. Lee and Seed (1967) updated the methodology of the cyclic triaxial testing of soils. Silver et al. (1977) defined the general approach and procedures belonging to cyclic triaxial testing. Chan (1981) has improved cyclic triaxial testing method and made it easier and faster to perform. Li, Chan and Shen (1988) designed a full-automated cyclic triaxial testing apparatus. The adoption of microprocessor-controlled loading

conditions and the use of electronic instrumentation for data acquisition and processing using test specific software have elevated the practice of laboratory testing in geotechnical engineering to a new level where the attention is focused on constitutive modelling of cyclic soil behaviour.

3.3 MECHANICS OF CYCLIC TRIAXIAL TESTING

3.3.1 Idealised In-situ Stress Conditions

The schematic stress conditions of a soil element under a level ground site are as shown in Figure 3.1.a. Under static conditions, the horizontal and vertical effective stresses on the element are defined as σ_v' and σ_h' respectively. Due to vertically propagating seismic shear waves during an earthquake, cyclic shear stresses, as shown in Figures 3.1.b and 3.1.c, will be imposed on the soil element.

3.3.2 Mechanics of Cyclic Triaxial Testing

If a saturated soil element, as shown in Figure 3.2.a, is consolidated under an all around pressure of σ_3 , the corresponding Mohr's circle will be as shown in Figure 3.2.b. Similarly, if cyclic deviatoric loads are applied such that the axial stress is equal to the $\sigma_3 + 0.5*\sigma_d$ and the radial stress is $\sigma_3 - 0.5*\sigma_d$ (Figure 3.2.c), and drainage into or out of the specimen is not permitted, then the corresponding Mohr's circle representation of this stress conditions will be as shown in Figure 2.2.d. Note that the stresses on the plane X-X are:

$$\text{Total normal stress} = \sigma_3$$

$$\text{Shear Stress} = 0.5* \sigma_d$$

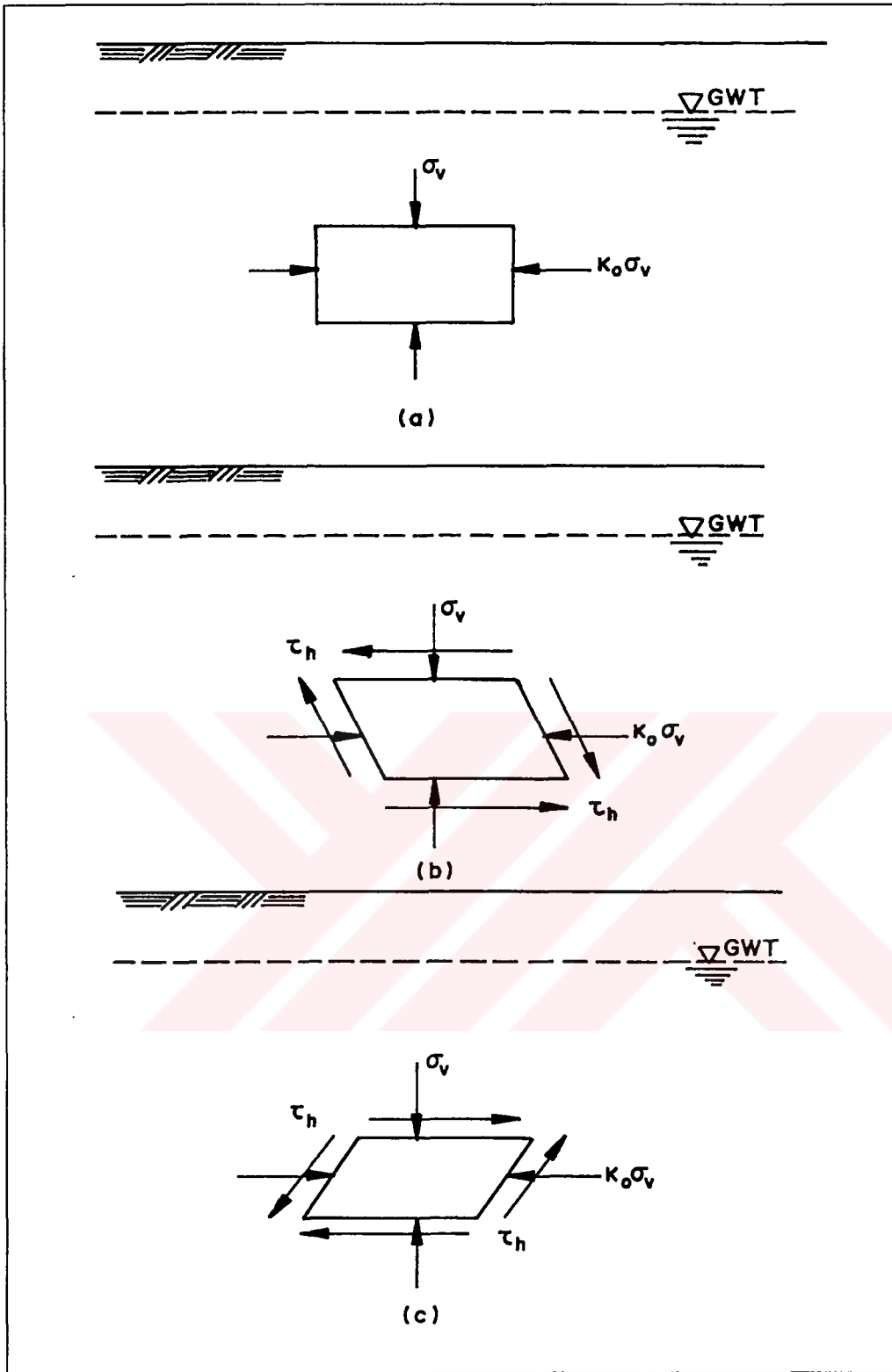


Figure 3.1 Illustration of Earthquake Induced Stresses on a Soil Element

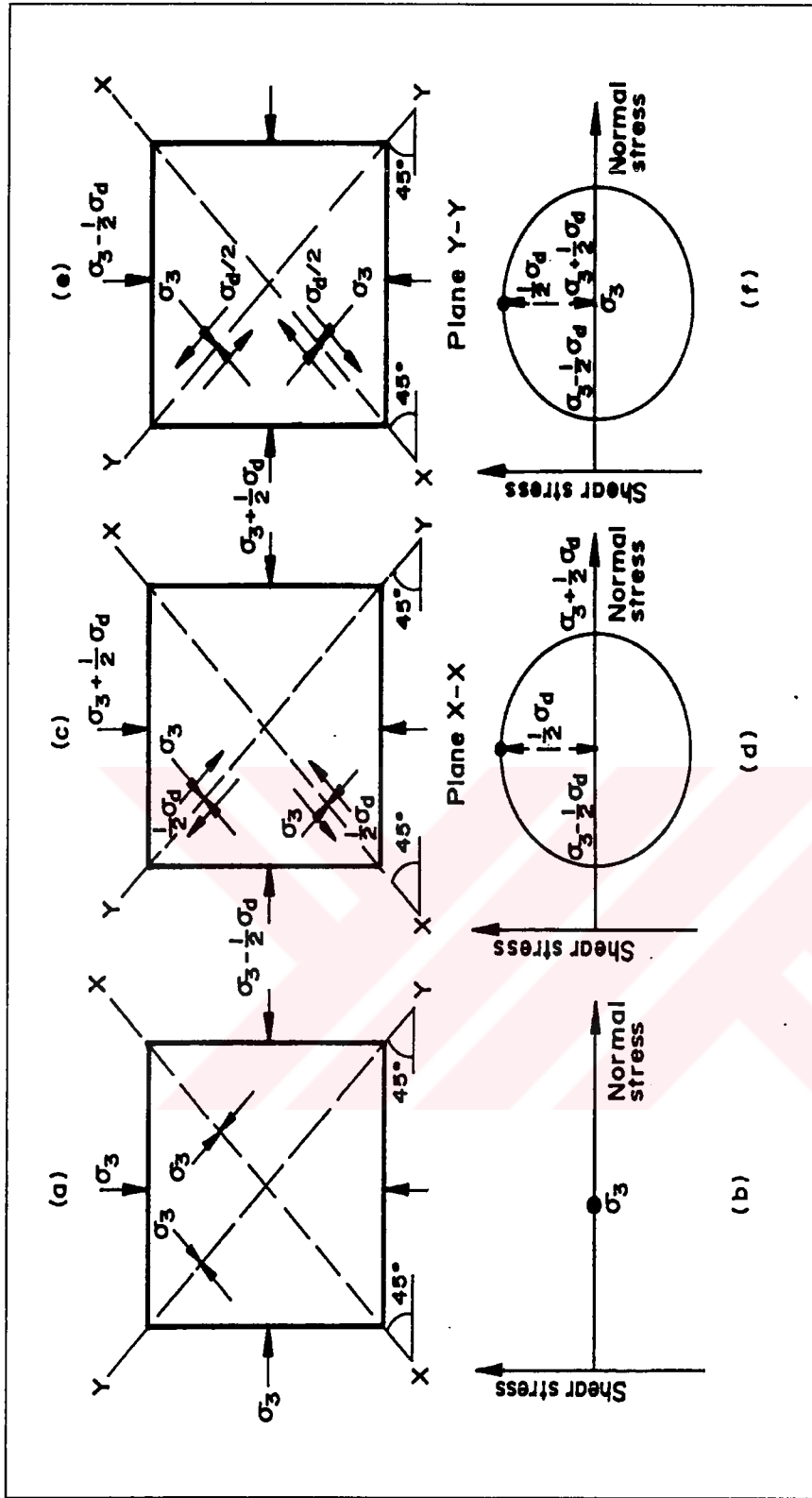


Figure 3.2 Simulation of Cyclic Shear Stress on a Plane for a Triaxial Test Specimen

and the stresses on the plane Y-Y are:

$$\text{Total normal stress} = \sigma_3$$

$$\text{Shear Stress} = -0.5 * \sigma_d$$

Similarly, if the deviatoric load is reversed, the stress conditions and Mohr's representation of it will be as shown in Figures 3.2.e and 3.2.f, respectively. The stresses on the plane X-X are:

$$\text{Total normal stress} = \sigma_3$$

$$\text{Shear Stress} = -0.5 * \sigma_d$$

and the stresses on the plane Y-Y are;

$$\text{Total normal stress} = \sigma_3$$

$$\text{Shear Stress} = 0.5 * \sigma_d$$

It is seen that, if the cyclic normal stresses of magnitude $0.5 \sigma_d$ are applied simultaneously in the horizontal or vertical direction, one can achieve a stress conditions along planes X-X and Y-Y that will be similar to the cyclic shear stress application shown in Figure 3.1.

In the laboratory, however, the test is conducted by applying an all around consolidation pressure of σ_3 and then applying a cyclic load having an amplitude of σ_d in the axial direction without allowing drainage as shown in Figure 3.3.a. The axial strain and the excess pore water pressure can be measured along with the number of cycles of deviatoric stress (σ_d) application. Note that the stress condition shown in Figure 3.3.b is the sum of the stress conditions shown in Figure 3.3.c and Figure 3.3.d. The effect of stress condition shown in Figure 3.3.d is to reduce the excess pore water pressure of the specimen by an amount $0.5 \sigma_d$ without causing any change in the axial strain. Thus the effect of stress conditions shown in Figure 3.3.b (which is the same as Figure 3.2.c) can be achieved by only subtracting a pore water pressure $u=0.5*\sigma_d$ from that observed loading condition

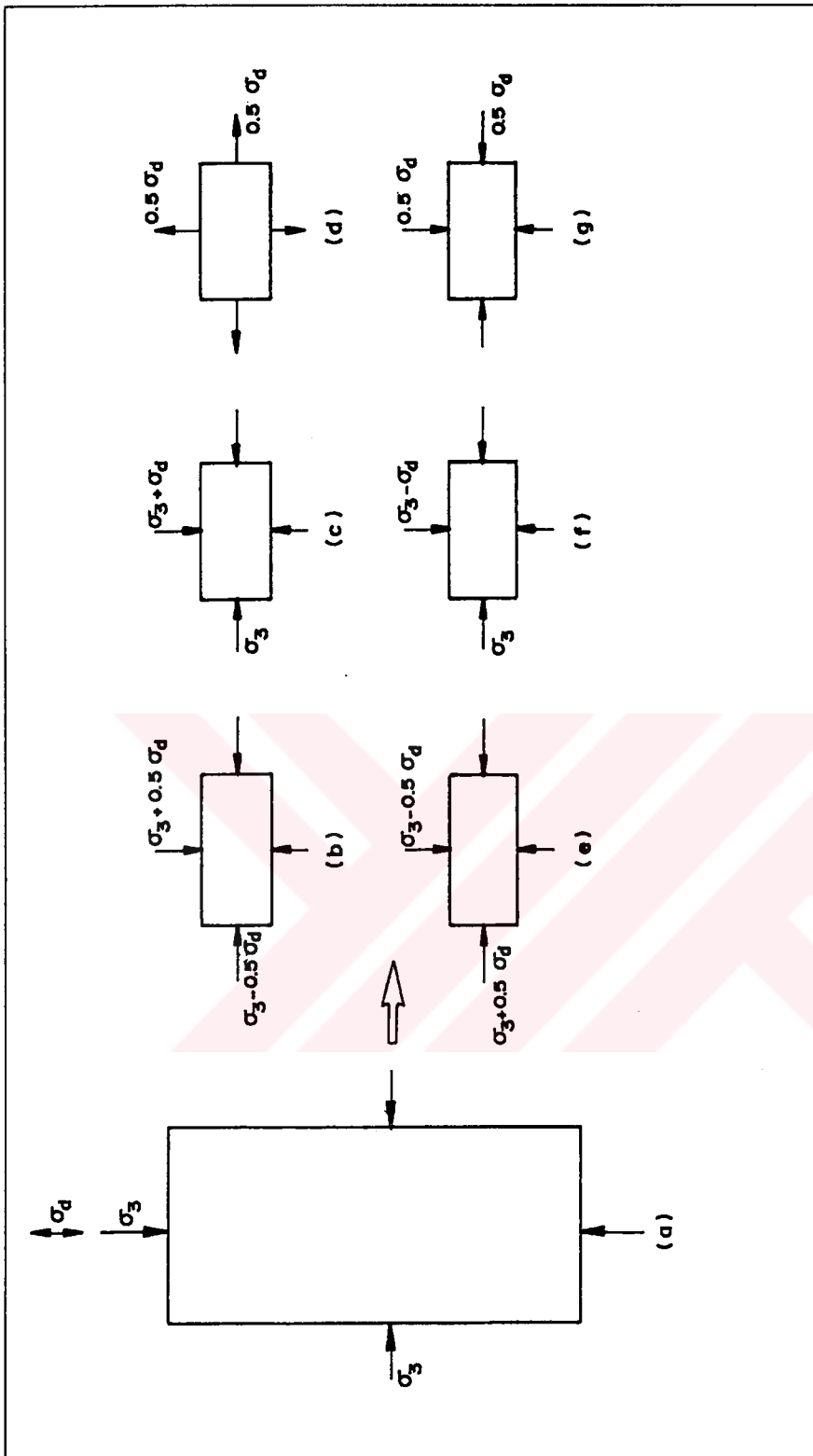


Figure 3.3 Simulation of Cyclic Triaxial Testing

shown in Figure 3.3.c. Similarly, the loading condition shown in Figure 3.3.e is the loading condition in Figure 3.3.f plus the loading condition in Figure 3.3.g. The effect of stress condition shown in Figure 3.3.g is only to increase the pore water pressure by an amount $0.5\sigma_d$. Thus the effect of the stress conditions shown in Figure 3.3.e (which is the same as in Figure 3.2.e) can be achieved by only adding $0.5\sigma_d$ to the pore water pressure observed from the loading condition in Figure 3.3.f.

3.4 ADVANTAGES AND LIMITATIONS OF CYCLIC TRIAXIAL TESTING

The advantages of the triaxial dynamic testing can be stated as follows:

- The stress conditions can easily be controlled.
- The pore water pressure, i.e., drainage conditions, can easily be controlled and measured.
- Any kind of soil property can be measured directly instead of assessment through theoretical analysis or empirical correlation.
- The measurement of axial and volumetric strains is relatively easy.
- The equipment is versatile, i.e., it may be used for a variety of determinations besides triaxial strength and stiffness (consolidation and permeability parameters and so forth).

Seed and Lee (1966) developed Cyclic Triaxial Test to provide a practical and convenient alternative for dynamic testing. However, its use requires the application of a correction factor to the results due to its limitations to simulate the in-situ loading conditions. Also, this test does not reproduce the correct initial stress conditions in the ground since it must be performed with an initially ambient pressure condition ($K_0=1$) to represent level ground conditions. Other limitations include:

- Stress concentrations at the cap and base of the test specimen
- 90° rotation of the direction of the major principal stresses during the two halves of the loading cycle
- Necking may develop and invalidate the test data beyond this point
- The intermediate principal stress does not have the same relative value during the halves of the loading cycle
- In the field, representative soil elements are subjected to multi-directional shaking whereas cyclic triaxial test simulates the uni-directional shaking

3.5 NORWEGIAN CYCLIC TRIAXIAL APPARATUS

The Norwegian cyclic triaxial apparatus has been used for cyclic testing of Adapazari soils. This type of triaxial testing apparatus is the most widely used dynamic testing device in geotechnical laboratories. It can be used to study soil response under both static and dynamic loadings. A general view of the apparatus is shown in Figure 3.4. The device, practical in design and versatile in control, is capable of performing tests of controlled stress rate of loading under both drained and undrained conditions. The system described here was mainly designed for studying the liquefaction potential and seismic mobility of soils and produced by Geonor under counsellor of the Norwegian Geotechnical Institute.

In the automated triaxial testing system, the computer-programmed electronic signal for frequency and magnitude of loading is applied to an electro-pneumatic transducer, which controls the pneumatic amplifiers for the application of loads. All modes of loading are controlled by manually, i.e., the parameters are controlled and checked against any mistakes by means observations. Although the system is designed for performing both, static and dynamic testing, only the latter

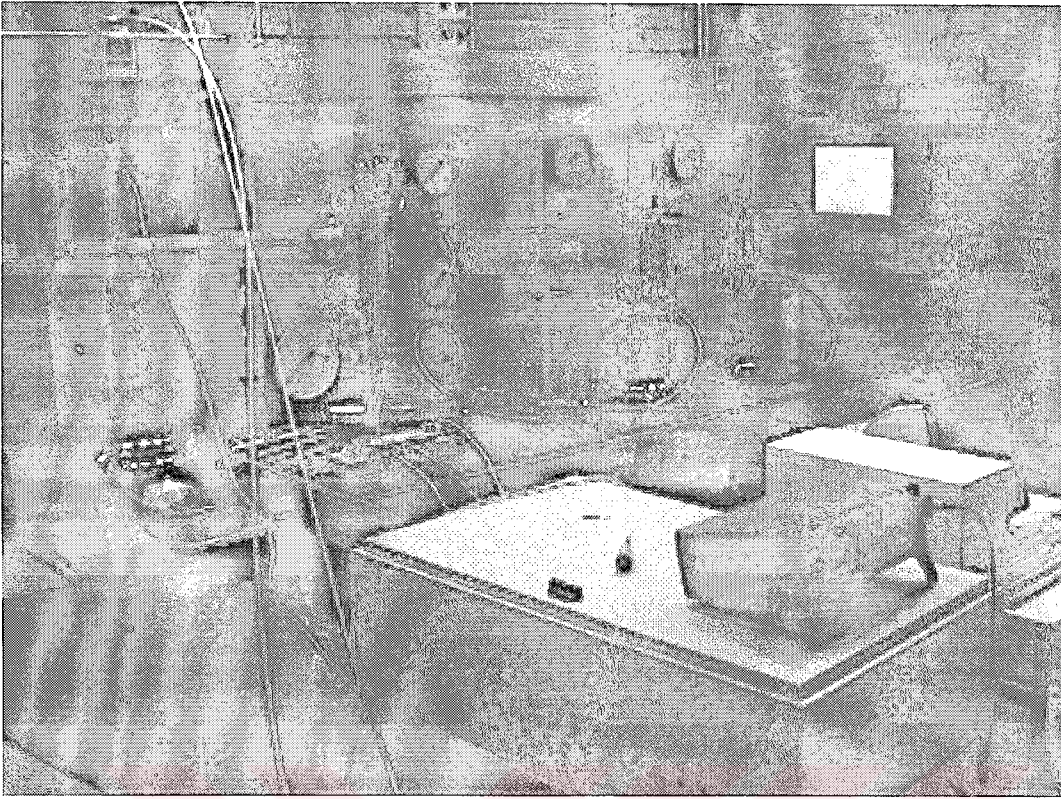


Figure 3.4 Norwegian Cyclic Triaxial Machine

one was implemented during this study. This system is best used for precision measurements of stress-strain relationships, for constitutive model calibration, for pore water pressure development under cyclic loading.

3.5.1 Cyclic Triaxial System Components

3.5.1.1 Triaxial Cell

The triaxial cell is equipped for a cylindrical specimen having 35.6 mm, but with adapters it can be modified for a specimen of 50 mm diameter. The cell is built with the low friction piston rod, three external tie rods, and straight through tube fitting on the pore fluid lines to the specimen cap and base.

3.5.1.2 Loading System Components

An electro-pneumatic system is used to convert the electronic command signal to pneumatic pressure, which in turn applies the axial load. The electro-pneumatic transducer essentially balances the force acting on the pneumatic tension-compression actuator, which applies a steady state cyclic pressure from the upper and lower air channels respectively. A screw handle on the air supply controls the back-pressure on lower side of the actuator. This is used for adjusting the load shape and magnitude.

3.5.1.3 Transducers and Signal Conditioner

A total of five sensors are used in the system. For the measurement of cell pressure and pore water pressure, the sensors having maximum capacities up to 10 bars and 16 bars are used, respectively. Error due to non-linearity is less than 0.1%. The volume change transducer can measure 50 cm³ of excess water. It has a non-linearity error of 0.25%. In general they are solid-state sensors and have good linearity. However, the ambient temperature is highly effective on the linearity of these sensors. In addition to these, the load gauge provides a continuous measurement of the force of the piston. It can measure both, tensile and compressive force up to 100 kilogram-force accurately when it is tightly fixed to system. Finally, the vertical displacement transducer used in the system is up to 50 mm and having 0.3% non-linearity. It has both electronic and visual read out.

The signal-conditioning unit accommodates five channels for five sensors, the load cell, the three pressure transducers and linear vertical displacement transducer. The output signals of these sensors are conditioned and then received by the process interface unit.

3.5.1.4 Process Interface Unit

The process interface forms the communication link between the computer and the loading sensor system. It is a compact and powerful unit, which can be used to interface with many different types of loading and measuring systems for material testing. The unit consists of a 16-channel, 12 bit, high-speed analog to digital (A/D) converter, 8 channels of 12 bit, high speed digital to analog (D/A) converters and 24 line digital input/output port.

3.5.1.5 Computer

The computer implemented in the system is a personal computer having 16 megabytes of ram and Pentium 133 main processor. It receives and stores real time data in its memory and issues control signals to regulate the test. The keyboard, mouse and display screen provide an effective and convenient means of communication between the operator and the testing system. The computer also performs other functions such as data processing by means of specific software.

3.6 GENERAL TESTING PROCEDURE

To simulate the field conditions during an earthquake, consolidated-undrained (CU) triaxial testing is performed. The sample is consolidated isotropically by applying a cell pressure, which is held constant during consolidation. After consolidation, water is forced through the drainage system under a slight pressure in order to remove any air bubbles and the pore pressure-measuring instrument is then connected to the cell and adjusted to read zero with its connection open to air. Both the pressures in the cell and the back-pressure, are increased simultaneously by the same amount so that the effective stress on the sample is equal to the in-situ value. At this stage, not to cause any over-consolidation, the back - pressure might be kept slightly larger than the cell

pressure. Back-pressure saturation continues until a satisfactory B value (>0.95) is achieved.

The deviator stress is calculated on the basis of average corrected cross sectional area of the sample at any stage of the test. The details of each step during cyclic testing will be discussed next.

3.6.1 Sample Preparation

3.6.1.1 Trimming the Sample

The samples were trimmed and placed in the testing apparatus immediately after being extruded from the sampling tube. The normal procedure was to cut samples by means of cylindrical pipes, which are 7.1 cm high and having 3.6 cm internal diameter, from tube, making sure that the end cuts are perpendicular to the vertical axis of the sample. The sample is, then, extracted by pushing a solid cylinder through the tubes. While one sample was being trimmed, the other was placed in the moist room or desiccator. Should it be necessary to postpone the trimming operation, the samples would be wrapped in the aluminium foil, labelled and sealed in wax while being careful not to allow the wax to penetrate into the specimen.

Under no circumstances should any pressure be applied to the sample. Therefore, it is best to transport the sample in the palm of the hand rather than just by fingertips. The sample is then weighed.

3.6.1.2 Placing the Filter Paper

The filter paper must be saturated to prevent absorption of moisture from the sample. Placing it in a firm of de-aired water saturates the paper. However there should be no free water on this paper. Next, the saturated paper should be

wrapped neatly around the sample, taking care not to trap any air bubbles beneath it. A slight finger pressure might be used to smooth out the filter.

3.6.1.3 Placing the Sample

The bottom plate is placed on the loading platform and the connections with the pore pressure and the cell pressure units are tightened. The back-pressure mechanism is also connected to the bottom plate and all of them are checked against leakage under high pressures, which might be up to 10 bars, while the valves on the bottom plate are closed.

The burette is filled with de-aired water up to some extent, usually 35 to 40 milliliters is preferred, and then connected to the bottom plate while the valve of volume change channel is closed. The bottom pedestal is lubricated with castor oil to guarantee the full coupling between the rubber membrane and the pedestal. Having checked that rubber membrane has no hole, it is put into the pedestal and two or three O-rings are placed around the rubber membrane so that there is no water leakage between the cell and the sample. The filter stone, which has been previously been boiled in water, is placed directly on the pedestal and inside the membrane. Then the rubber membrane is placed in the mounting cylinder and slight suction is applied to hold the membrane tight against the walls of the cylinder while the membrane being smooth and not twisted. The volume change valve is then opened and de-aired water is circulated through the system until the pore pressure channel is saturated. At this stage, the value of the pore pressure on the program should be set to zero before connecting the pore pressure pipe to the transducer. Having checked that the water level is exactly at the top of the filter stone, then the volume change valve is closed. Then the sample is placed in the rubber membrane (still holding the membrane tight with vacuum). Another filter stone is placed at the top of the sample. Then the back-pressure mechanism is saturated before the top cap, with lubricated ends, is placed over the filter stone. The rubber membrane is then picked upwards. Two O-rings are then placed

around the top cap to prevent leakage into the sample. Up to this stage, one should be careful about the fact that the rubber membrane should not be punctured.

The diameter of the specimen at both ends and middle of the sample and the height of the sample are measured before positioning the top section of the triaxial cell. When lowering this unit over the sample, the piston must be held up so that it does not press on the sample. The upper cell section is rotated until the three wing bolts line up with the holes in the bottom plate. Having tightened these bolts in such a manner that the top and the bottom plates are parallel let the piston fall into the socket of the loading cap; it may be necessary to tilt the entire cell in order to assure its alignment. Then, the cell is filled with water after opening the screw valve to allow the entrapped air to escape.

3.6.2 Sample Consolidation

3.6.2.1 Developing the Desired Cell Pressure

Before applying the cell pressure, the cell pressure valve on the bottom plate is closed against any fluctuations in the pressure. The connection valve between the screw control and the tap water is opened, then the screw control is filled by turning it almost all the way out. The tap water connection is then closed. The pressure caused by the weights is checked after the piston has been given a slight movement by the screw control. The load is adjusted and the pressure is checked again as mentioned above until the desired pressure is reached.

The valve to the constant pressure cell is closed and the desired cell pressure in the triaxial cell is built up with the screw control. The valve to the constant pressure cell is opened and with this the system is ready for consolidation.

3.6.2.2 Consolidation of the Specimen

The lock that prevents the movement of the rod connecting the load cell to the sample is opened to allow the volumetric expansion or consolidation. The initial water level in the burette is recorded against possible electricity shortage during consolidation. Having all these steps completed, the recording is started, and the volumetric change and cell pressure valves are opened to start consolidation.

Due to prolonged consolidation process, cell pressure may slightly drop because of leakage in the system. In such cases, the connection to the triaxial cell is closed and the constant pressure piston is pushed upwards again by means of the screw control. The valve to the triaxial cell is opened is back as soon as the pressure is stabilized at the desired level.

3.6.3 Sample Saturation

After consolidation is completed, the recording is stopped and the valve to the volumetric change is closed, the final water level in the burette is recorded. The lock of the piston is again closed against any disturbance. To remove the air from the filter stone and its connections, the connection to the pore pressure is loosened and the back-pressure valve and volume change valve are opened and water is circulated under a slight pressure. The saturation is checked through inspection of the water coming from the connection of the pore water pressure line. The visual inspection and consecutive removal of the air bubbles in the plastic pipes is also necessary in the system. It is important to connect the pipe to the transducer while the water is flowing out.

Having been sure that the system, not necessarily the specimen, is fully saturated, the saturation process of the specimen can be started. For this purpose the cell pressure outside the specimen and the back pressure inside the specimen

are increased by means of the screw control while the effective stress is held constant, at a level slightly less than the desired one, not to over-consolidate the specimen. The important point while saturating the specimen is that the effect of any increase or decrease in pressure in the system can be observed after sometime, because the variation in pore pressure is to be distributed uniformly throughout the specimen. In other words, the pore water pressure is to be stabilized within the sample. Stabilization of the pore pressure can be checked through the mercury manometer connected to the back-pressure mechanism of the system.

The second important point is that any change in any one of the pressures is to be stabilized following application to the system. Therefore the valves to the corresponding mechanisms are to be closed. Moreover, the amount of increase in the back-pressure values should be small while the cell pressure around the specimen is small. Back-pressure value can be increased as the value of the cell pressure is increased. This procedure should be applied, because at small values of cell pressure, i.e., around 1 to 2 bars, the pore pressure of the specimen is not responsive considering the frequency of loading. The possible reason behind this is the trapped air in the system. On the other hand, at high pressures (ie. greater than 3 bars), the trapped air existing on the system is resolved in the water.

Examining pore pressure coefficient, B , can check the saturation of the specimen. This coefficient is used to express the response of pore water pressure to change in total stress under undrained conditions. To evaluate B , under any value of all-round pressure, the existing pore water pressure is recorded first. Under undrained conditions, the all-round pressure is then increased (or reduced) by an amount $\Delta\sigma_3$ and the change in pore water pressure (Δu) from the initial value is measured, enabling the value of B to be calculated from Equation 3.1.

$$B = \frac{\Delta u}{\Delta \sigma_3} \quad (3.1)$$

When the value of B gets higher than 0.95, then the system is said to be saturated. For silty soils the value of B generally gets easily higher than 0.95, however, for clayey soils it is quite difficult to achieve a B value higher than 0.95.

3.6.4 Calibration

Before starting the experiment, the data acquisition of the system should be turned on so that the connections between the transducers' signals and data

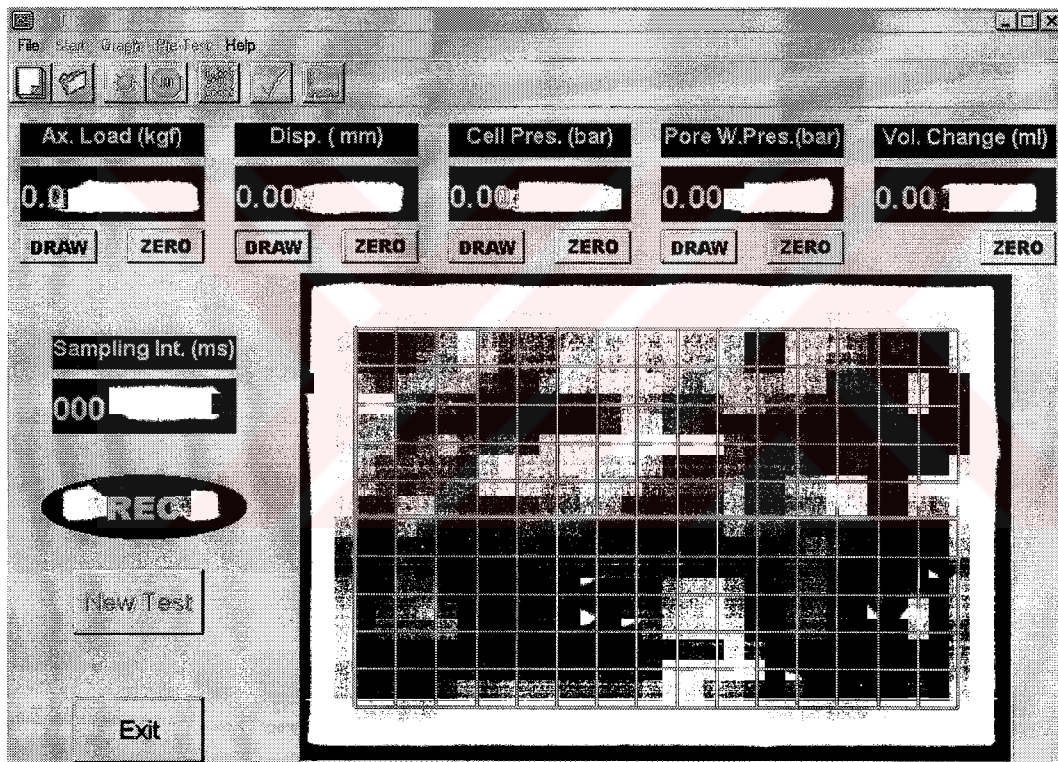


Figure 3.5 TLT Interface

logging system adapt with the room temperature. It is best to open this system at least 10 minutes before the experiment starts.

The computer program Triaxial Loading Test (TLT) (Figure 3.5) has to be run to see the numerical outputs of the voltages coming from transducers. For this purpose, the setup icon of the program is clicked. The calibrations of all the electronic devices are to be done from this screen.

Since there is no need for the pore water pressure measurement during consolidation, the calibration of the volumetric change and the cell pressure transducers was done next. This operation can be achieved by changing the value of B, i.e., the offset of the transducer, on the screen and adjusting the output numerical value to zero while the corresponding transducers' connection is open to air. The screen of transducer calibration is shown on Figure 3.6.

3.6.5 Cyclic Testing

3.6.5.1 Assembling the Force Transducer and the Displacement Gauge

The load cell is set up on the specimen while the loading bar is locked. To get satisfactory B values for saturation, usually high values of cell pressure are to be applied in the experiments. However this causes the net force, resulting the specimen to displace, on the specimen to deviate from zero. To overcome this discrepancy, additional dead weights are hanged on the system when the cell pressure is greater than 1.94 bar. This value is found from the net force calculations, which are based on the dead weights in the gravity direction and the cell pressure in the upward direction, which is converted to force value in calculations and the friction existing on the system. (The frictional force acting on the system is calculated based on calibration tests.)

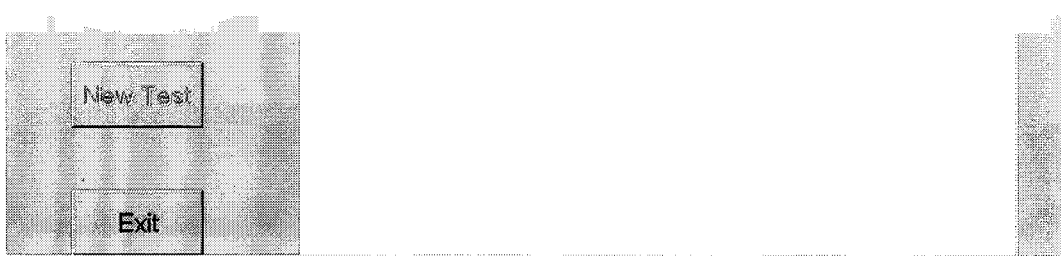


Figure 3.6 Calibration Interface of TLT

The air valve of the actuator is opened and the power function generator is turned on to release the air stored in the system before coupling the load cell mechanism to the actuator. By turning the back-pressure valve to right or left on the control unit of the system, the tip of the actuator is set to a suitable starting position for cyclic loading so that the Mohr Circle shifts right and left during the corresponding cycles of loading. The load cell reading on the program is set to zero while it is just in contact with the actuator.

As the displacement gage is attached to the system, its reading is taken care to indicate almost the mid-point of the range. This is done because the gage is most sensitive around the center of its range, i.e., between 10 and 25 mm. The displacement level on the program is set to zero just before starting the

experiment. This is necessary to activate the recording of the program. It is important to position the displacement gage parallel to the axis of the triaxial cell.

3.6.5.2 Starting the Test

Just before starting the test, all the valves on the triaxial cell are closed except the valve connecting the cell pressure, which provides a constant level of pressure in the cell. Furthermore, during testing loading rod is adjusted at half of its travel range so that it acts with its best efficiency.

The power function generator is set to “run” position while keeping the magnitude of the load at zero. Since the pressure regulator on the control unit sometimes leaks air before initiation of the test, the desired load value is re-checked on the triaxial cell while the loading rod is locked. This is also necessary to see the noise existing on the system. If the load is not symmetric with respect to the horizontal axis, then the load is set to zero in the power function generator and the shift is set to zero by turning the back pressure valve on the control unit manually.

The output file name is entered to the program with an extension of .out, so that the readings of the transducers are recorded and saved to this output file. When this information is entered to the program, the recording is activated through the button on the program menu.

3.6.5.3 During the Test

The loading rod is unlocked so that the load from the activator starts acting on the specimen. Then, the test is started and the pore pressure variation, the accumulated displacement and the load variation, are observed during the test.

During testing accumulated displacements on the specimen causes a small amount of shift in the symmetry and magnitude of the load. Adjusting the offset level on the power function generator, which was zero at the beginning of the test, can prevent this.

3.6.5.4 Unloading and stopping the test

The power function generator is set to zero while keeping the air supply on the system. The system is locked against any disturbances of the specimen. To simulate the post earthquake behaviour, the cell pressure is decreased to the level anticipated to have existed in the static case, ie. before the earthquake. Simultaneously, the valve of the volume change is opened so that the generated pore pressure and the volume of the specimen decreases. When the pore pressure in the specimen reaches to stability, the recording is stopped.

3.6.5.5 Removing the Sample

The pressure in the triaxial cell is reduced. All the valves are closed and the plastic pipes are removed from their connections to the triaxial cell. The screw valve at the top of the cell is loosened and the water is emptied through cell pressure valve to a container. The connection between the actuator and the loading rod is loosened. Then the wing bolts are loosened and the upper section of the cell is removed.

The upper part of the rubber membrane is folded over O rings. The rings are then rolled off and the top cap on the sample is detached. The rubber membrane is straighten out again and pulled down the sample.

3.7 LABORATORY DATA CORRECTION

Due to the limitations of cyclic triaxial testing as discussed in section 3.4, the laboratory data should be corrected for better representing field conditions. Corrections for incorrect planes tested and bi-directional loading will be discussed next.

3.7.1 Incorrect Planes of Failure

The main cause for a correction of laboratory data is that the planes that are sheared during undrained cyclic triaxial testing are $\pm 45^\circ$ planes to the horizontal. However due to the vertically propagating seismic shear waves, horizontal planes are sheared at level sites during an earthquake. Thus, applied deviatoric stress need to be corrected to account for the error in testing different planes. In the literature a correction in the form as given in Equation 3.2 is recommended.

$$\left(\frac{\tau_h}{\sigma'_0}\right)_{shear} = C_r * \left(\frac{\sigma_d}{2 * \sigma'_3}\right)_{triaxial} \quad (3.2)$$

The suggested values for C_r are summarized in Table 3-1.

Table 3-1 Recommended C_r Values For Various Field Conditions

	C_r	$K_0=0.4$	$K_0=1.0$
Finn et al. (1970)	$(1 + K_0) / 2$	0.7	1.0
Seed and Peacock (1971)	Varies	0.55 to 0.72	1.0
Castro (1975)	$2 * (1 + K_0)$	0.69	1.15

A value of 0.72 was adopted for C_r within the scope of these studies. Similarly, during cyclic triaxial testing, deformations (strains) are recorded only in the vertical direction. These axial strains are to be converted to shear strains for the purpose of estimating shear stiffness. The cyclic triaxial test based axial strains can be used to estimate cyclic simple shear, similar to seismic field conditions. Cyclic simple shear strain, γ_{cy} , is related to the cyclic triaxial axial strain by ε_{cy} by either of two similar expressions (Vucetic and Dobry, 1991):

$$\gamma_{cy} = 1.5 * \varepsilon_{cy} \quad (3.3)$$

$$\gamma_{cy} = \sqrt{3} * \varepsilon_{cy} \quad (3.4)$$

Within the scope of this study, axial strains were converted to simple shear strains by Equation 3.3.

3.7.2 Bi-direction Loading Effects

In the laboratory test results, if the apparatus is not designed to apply bi-directional loads, there needs to be a correction made to take into account, the bi-directional loading of earthquakes, under in-situ conditions. Pyke et. al. (1975) suggested a value of 0.9 for this correction as given in Equation 3.5.

$$\left(\frac{\tau_h}{\sigma_0}\right)_{in-situ} = 0.9 * \left(\frac{\sigma_d}{2 * \sigma_3}\right)_{triaxial} \quad (3.5)$$

CHAPTER 4

INTERPRETATION OF RESULTS

4.1 INTRODUCTION

This chapter presents the results of a total of 11 cyclic triaxial tests performed on selected silty clay or clayey silt Adapazari soils. The findings were summarized in the form of cyclic stress ratio versus number of cycles for both 3% and 7.5% shear strains. As a conclusion, variability in certain characteristics of samples such as void ratio, PI, etc. was questioned to be possible explanations for observed differences in cyclic behaviour.

4.2 CYCLIC TRIAXIAL TEST RESULTS

For each sample tested, engineering properties including Atterberg limit tests, gradation curves with hydrometer tests were performed. Similarly, the results of cyclic tests were chosen to be presented in four identically scaled figures of;

- i. Normalized effective mean stress versus cyclic stress ratio (CSR)
- ii. Number of cycles versus excess pore pressure ratio
- iii. Shear strain versus CSR
- iv. Shear strain versus number of cycles

These four scaled plots enabled us to observe strain and cycle dependent variation of stiffness and effective stress (pore pressure). Additionally, cycles to liquefaction (in this study, it is defined as either 100% pore pressure generation or

5% double amplitude axial strain which also correspond to 7.5% shear strain) or the dilation and contraction behaviours after liquefaction can also be clearly identified by the use of these 4 plots. Note that the “CSR versus number of cycles” graphs are presented in terms of 7.5% and 3% shear strains. These values are arbitrarily selected to explain the foundation displacements observed in Adapazarı and for studies considering the displacements depending on the importance of structures.

4.2.1 Definitions of Terms Used in 4-way Graphs

In this study normalized effective mean stress (p') is defined as:

$$p' = \frac{\sigma_3 + \frac{\sigma_d}{2} - u}{\sigma_{3,initial} - u_{initial}} \quad (4.1)$$

where

σ_3 is the constant cell pressure

σ_d is the deviatoric stress

u is the pore pressure

$(\sigma_{3,initial} - u_{initial})$ is the normalization factor in which $\sigma_{3,initial}$ is the initial cell pressure and $u_{initial}$ is the initial pore water pressure.

The deviatoric stress on the sample is calculated from the following formula.

$$\sigma_d = \frac{F_{applied}}{A_{corrected}} \quad (4.2)$$

where

$F_{applied}$ is the applied cyclic load on the specimen

$A_{corrected}$ is the corrected cross sectional area

Since the cross sectional area of the specimen during testing does not remain constant, the area of the specimen during testing is corrected as follows.

$$A_{corrected} = \frac{A}{1 - \varepsilon_{cy}} \quad (4.3)$$

where

A is the initial cross sectional area of the specimen

ε_{cy} is the cyclic triaxial axial strain developed in the specimen

The cyclic triaxial axial strain is calculated from the following formula;

$$\varepsilon_{cy} = \frac{\delta L}{L_0 * 100} \quad (4.4)$$

where

δL is the change in height with respect to initial height

L_0 is the initial height

The calculation of cyclic simple shear strain accumulated on the specimen is given in Chapter 3.

In the Mohr's Circle statement of the stresses for cyclic triaxial testing, the shear stress is half of the deviatoric stress.

$$\tau = \frac{\sigma_d}{2} \quad (4.5)$$

where

F_{shear} is the shear force on the specimen

$A_{corrected}$ is the corrected cross sectional area of the specimen

Based on the above formula the cyclic stress ratio (CSR) is calculated as follows:

$$CSR = \frac{\tau}{\sigma_{3,initial} - u_{initial}} \quad (4.6)$$

The pore pressure ratio (r_u) is defined as follows:

$$r_u = \frac{u - u_{initial}}{\sigma_{3,initial} - u_{initial}} \quad (4.7)$$

The specifics of each individual test will be discussed next.

4.2.2 Site C

Two tests were performed on the samples retrieved from depths of 3.49 m (C1-1) and 3.69 m (C1-3) with the engineering properties as summarized in Table 4-1, Figure 4.1, Table 4-2 and Figure 4.3, respectively.

As shown in Figure 4.2, the sample of C1-1, as a result of applied deviatoric load expressed in terms of a $CSR_{in-situ}$ of 0.35, can be concluded as not liquefied after 700 cycles if 100% pore pressure ratio-based liquefaction definition is adopted. However, after 700 cycles 5% double amplitude axial strain is well developed. The slow pore pressure generation behaviour is not surprising since the sample C1-1 is defined as fat clay (CH) with clay content of 37% and PI, 35%. However, as these test results have shown, clays can liquefy (both, in the sense of pore pressure generation and threshold strain) under cyclic loads if enough cycles are produced.

Table 4-1 Engineering Properties of Specimen C1-1

Borehole ID	SPT-C1	Sample ID	C1-3 / UD-1
Specimen ID	C1-1	Depth of Specimen (m)	3.49 (3.45-3.52)
Depth to Water Table (m)	1.4	Liquid Limit (%)	58
G_s	2.57	Plastic Limit (%)	23
Water Content (%)	39	Plasticity Index (PI)	35
Fines Content <0.074mm (%)	97	Clay Content <0.002mm (%)	37
C_u	N/A	C_c	N/A
Initial Void Ratio	1.01	Final Void Ratio	0.95
B Value	0.95		
Unified Soil Class.	Fat Clay (CH)		

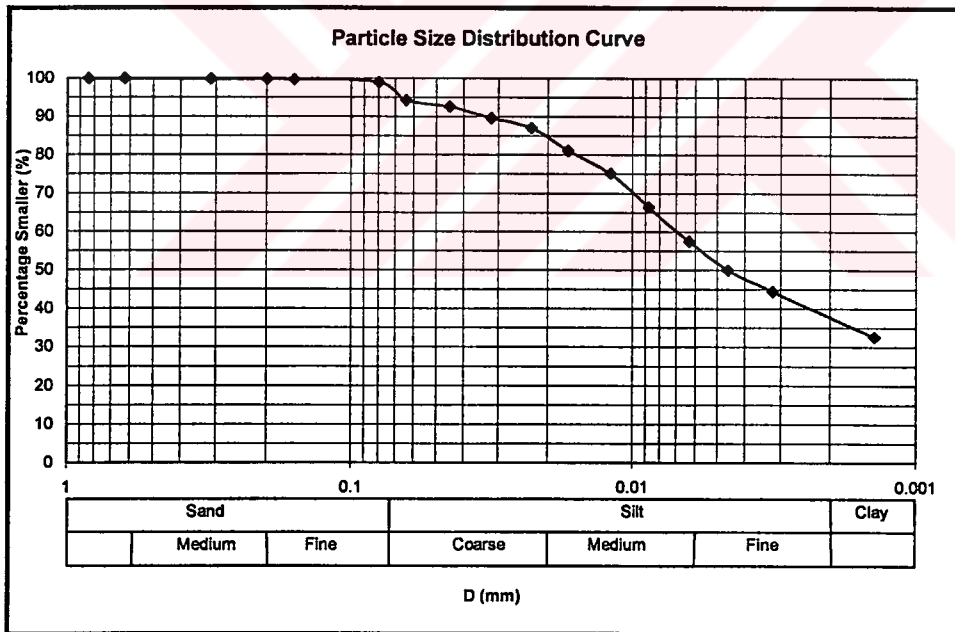


Figure 4.1 Particle Size Distribution for Specimen C1-1

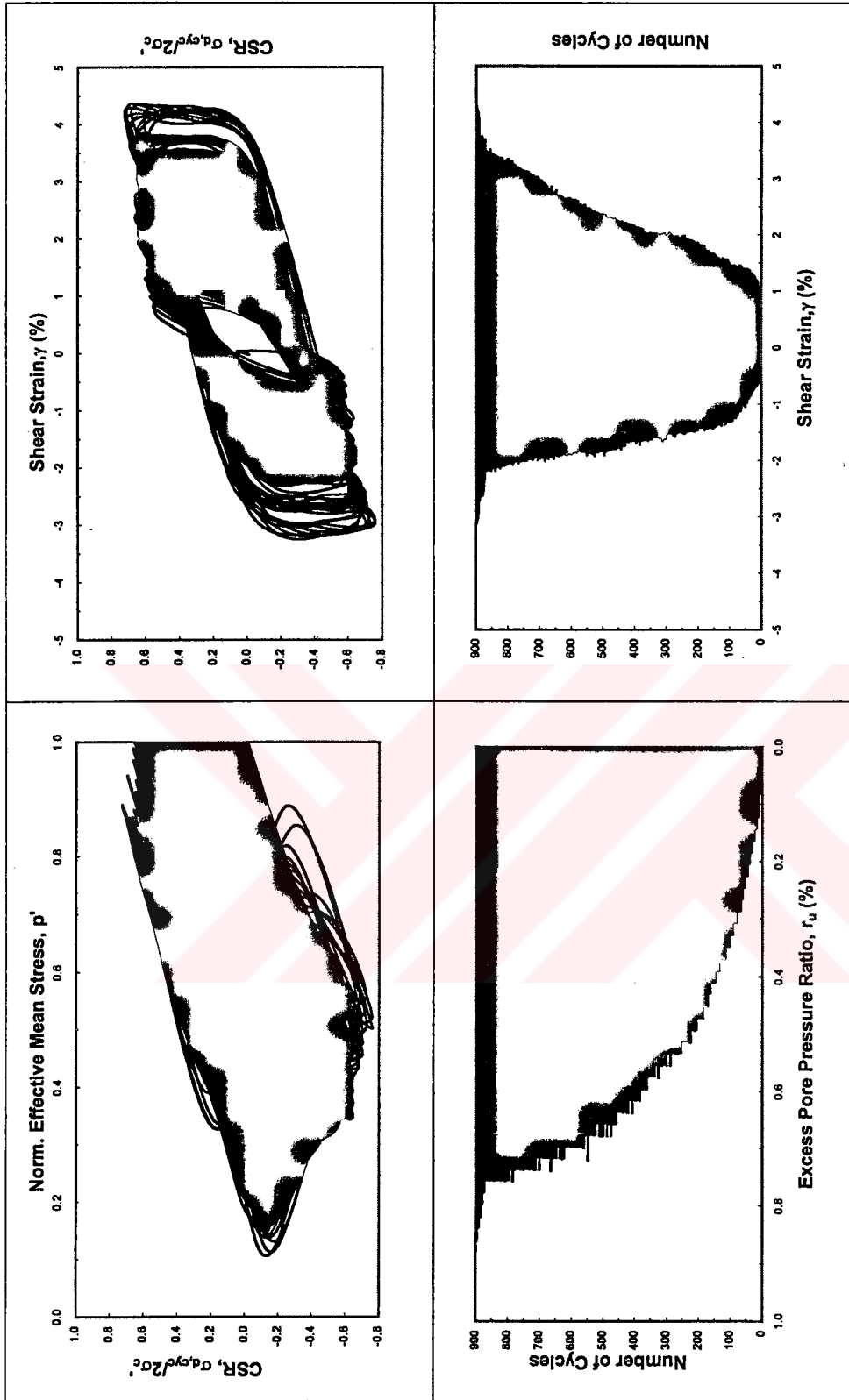


Figure 4.2 CTX Results for Specimen C1-1

Table 4-2 Engineering Properties of Specimen C1-3

Borehole ID	SPT-C1	Sample ID	C1-3 / UD-1
Specimen ID	C1-3	Depth of Specimen (m)	3.69 (3.65-3.72)
Depth to Water Table (m)	1.4	Liquid Limit (%)	34
G_s	2.57	Plastic Limit (%)	25
Water Content (%)	36	Plasticity Index (PI)	9
Fines Content - <0.074mm (%)	93	Clay Content - <0.002mm (%)	23
C_u	N/A	C_c	N/A
Initial Void Ratio	0.94	Final Void Ratio	0.89
B Value		0.96	
Unified Soil Class.		Lean Clay (CL)	

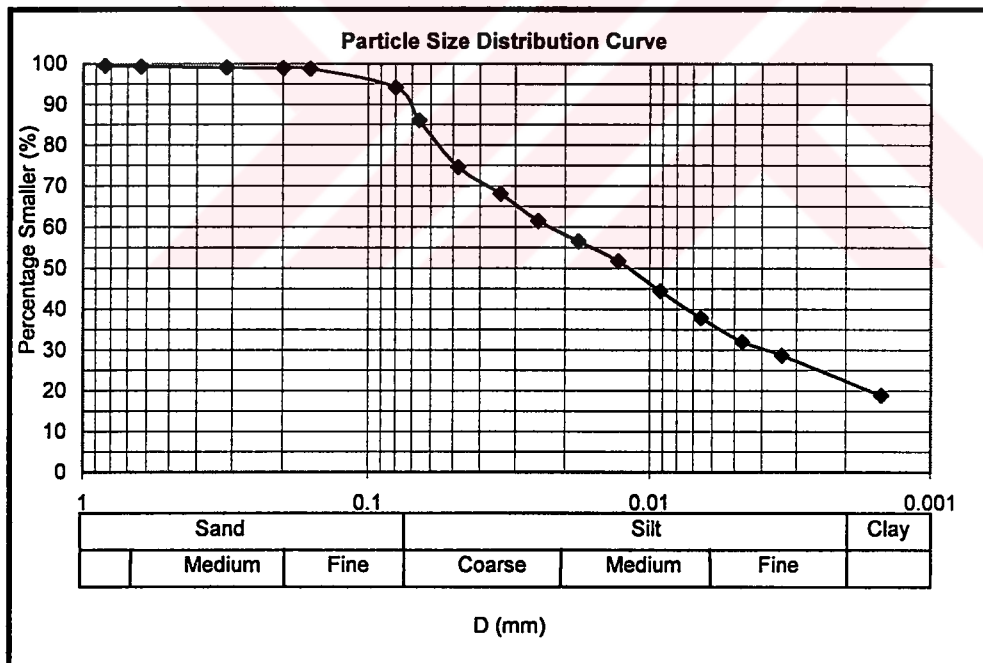


Figure 4.3 Particle Size Distribution for Specimen C1-3

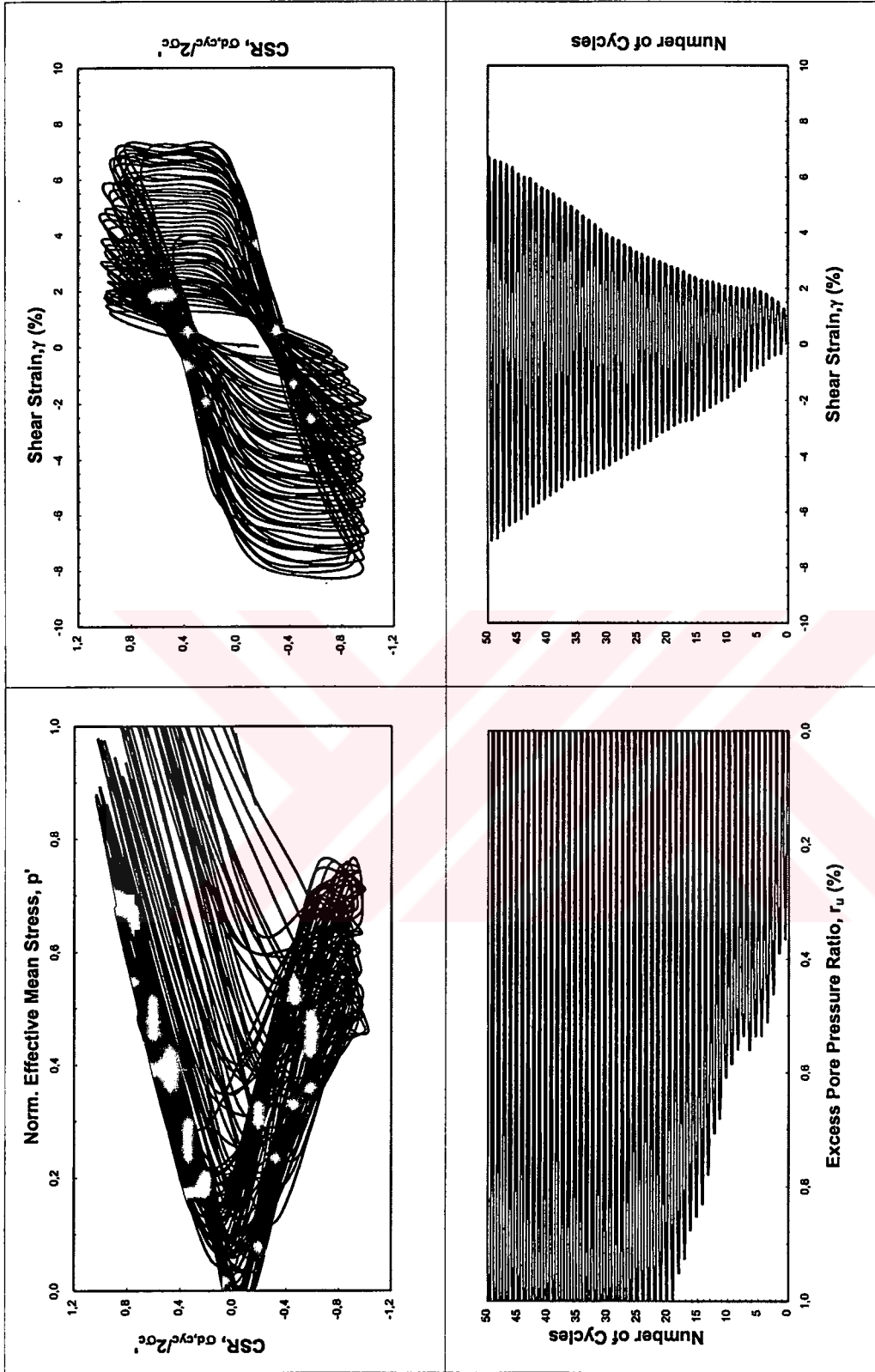


Figure 4.4 CTX Results for Specimen C1-3

Figure 4.4 presents the results of cyclic triaxial tests performed on sample C1-3. As it is clearly seen on “number of cycles versus excess pore pressure ratio” plot, sample develops 100% pore pressure at about 18th cycle of applied CSR of 0.56. Even though this sample is classified as lean clay (CL) based on soil classification, it was proved through this test that it can surely be liquefied at very similar CSR’s and number of cycles to those anticipated (Bakır et. al., 2002) to have liquefied during İzmit Earthquake in Adapazarı.

Figure 4.5 summarizes the results of cyclic triaxial tests performed on samples acquired from site C. Both 3% and 7.5% shear strain based CSR vs. Number of cycles plots are shown. As can be clearly seen from this figure that as a result of similar shaking intensity and duration to those recorded in Adapazarı after İzmit earthquake, foundation soils can easily accumulate 3 - 4 % shear strain (corresponding to 1.5 - 2% axial strain).

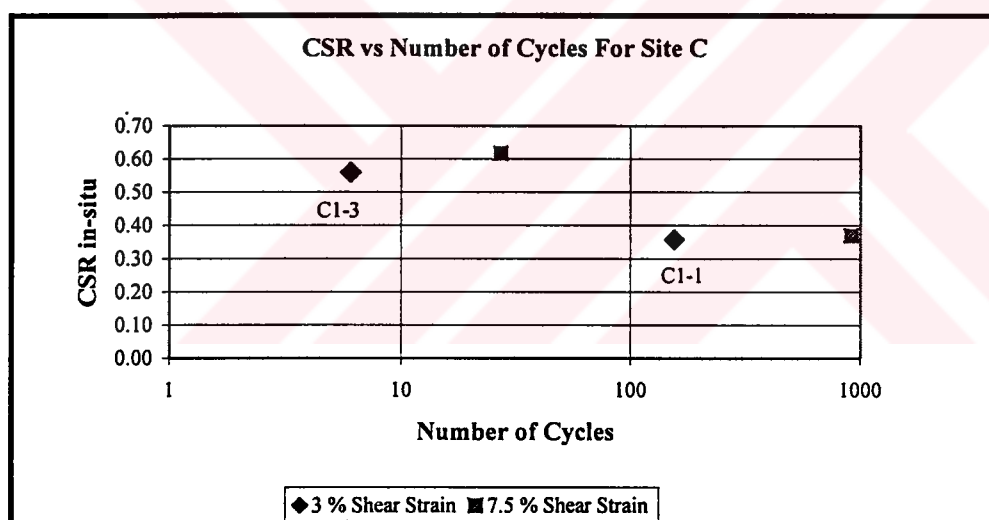


Figure 4.5 CSR vs. Number of Cycles For Site C

4.2.3 Site D

Two tests were performed on the samples retrieved from depths of 1.54 m (D2-1) and 1.64 m (D2-2) with the engineering properties as summarized in Table 4-3, Figure 4.6, Table 4-4 and Figure 4.8, respectively.

As shown in Figure 4.7, the sample of D2-1, as a result of applied deviatoric load expressed in terms of a $CSR_{in-situ}$ of 0.39, can be concluded as non-liquefied after 35 cycles if 100% pore pressure ratio-based liquefaction definition is adopted. However, after 15 cycles 5% double amplitude axial strain (7.5% shear strain) is well developed. The pore pressure generation behaviour is very similar to those of silts and sands, since, even though the sample D2-1 is defined as lean clay (CL) with clay content of 15% and PI of 7%. Once again, as these test results have shown, clays can liquefy (both in the sense of pore pressure generation and threshold strain) under cyclic loads if enough cycles are produced.

Figure 4.9 presents the results of cyclic triaxial tests performed on sample D2-2. As it is clearly seen on “number of cycles versus excess pore pressure ratio” plot, sample develops significant pore pressure ($r_u > 0.5$) at early stages of cyclic loading expressed in a value of CSR of 0.39. Even though these samples are classified as lean clay (CL) based on soil classification, and they are assumed to be not vulnerable to liquefaction, it was proven through this test that they can surely liquefy at very similar CSR's and number of cycles to those anticipated during İzmit Earthquake.

Figure 4.10 summarizes the results of cyclic triaxial performed on samples acquired from site D. Both 3% and 7.5% shear strain based CSR versus number of cycles plots are shown. As can be clearly seen from this figure that as a result of similar shaking intensity and duration to the ones recorded in Adapazarı after İzmit earthquake, foundation soils can easily accumulate 5-7.5% shear strain (corresponding to 3.5-5% axial strain).

Table 4-3 Engineering Properties of Specimen D2-1

Borehole ID	SPT-D2	Sample ID	D2-1 / UD-1
Specimen ID	D2-1	Depth of Specimen (m)	1.54 (1.50-1.57)
Depth to Water Table (m)	1.4	Liquid Limit (%)	30
G_s	2.58	Plastic Limit (%)	23
Water Content (%)	32	Plasticity Index (PI)	7
Fines Content - <0.074mm (%)	72	Clay Content - <0.002mm (%)	15
C_u	N/A	C_c	N/A
Initial Void Ratio	0.86	Final Void Ratio	0.78
B Value		0.96	
Unified Soil Class.		Lean Clay (CL)	

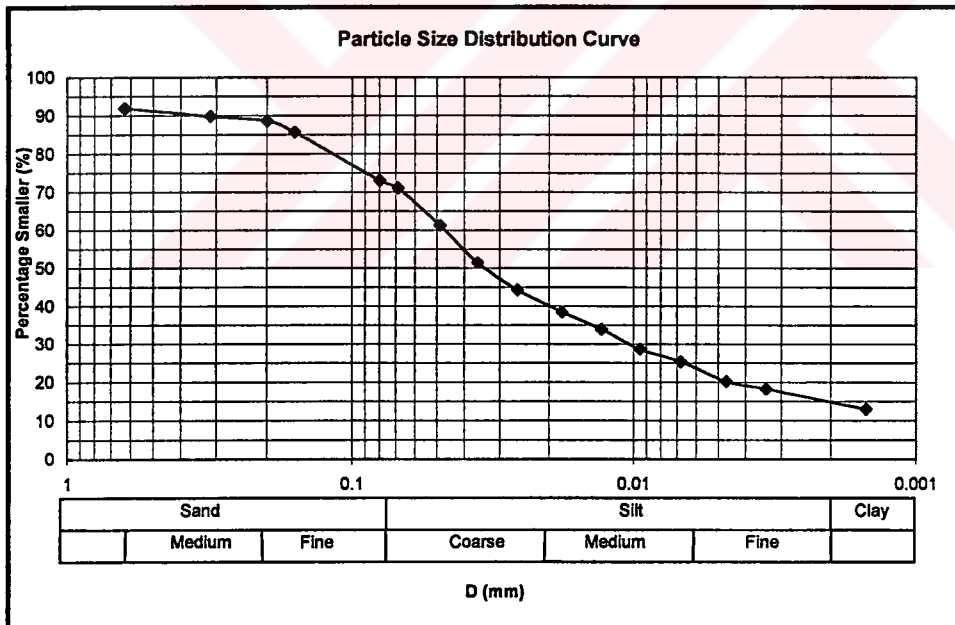


Figure 4.6 Particle Size Distribution for Specimen D2-1

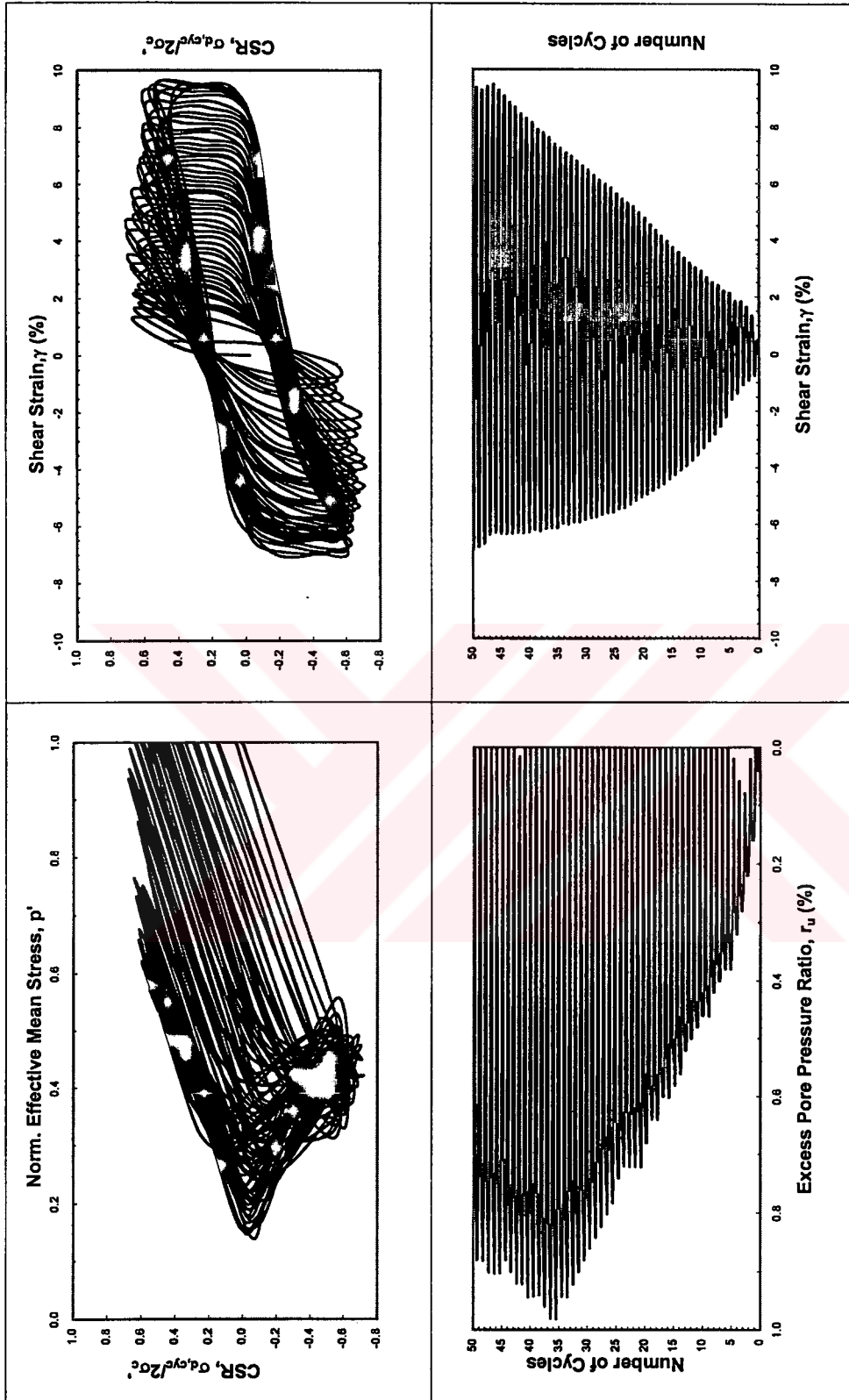


Figure 4.7 CTX Results for Specimen D2-1

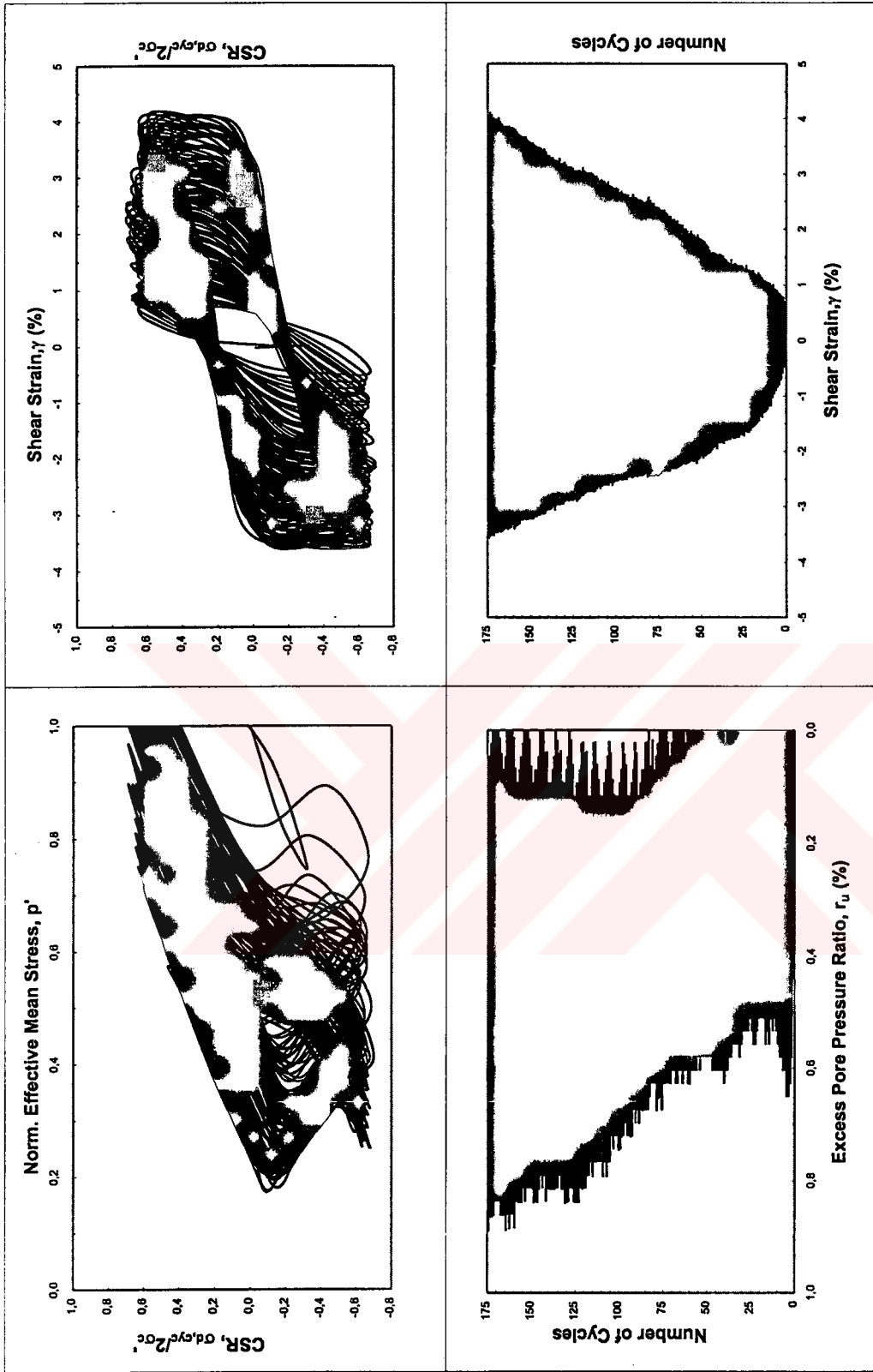


Figure 4.9 CTX Results for Specimen D2-2

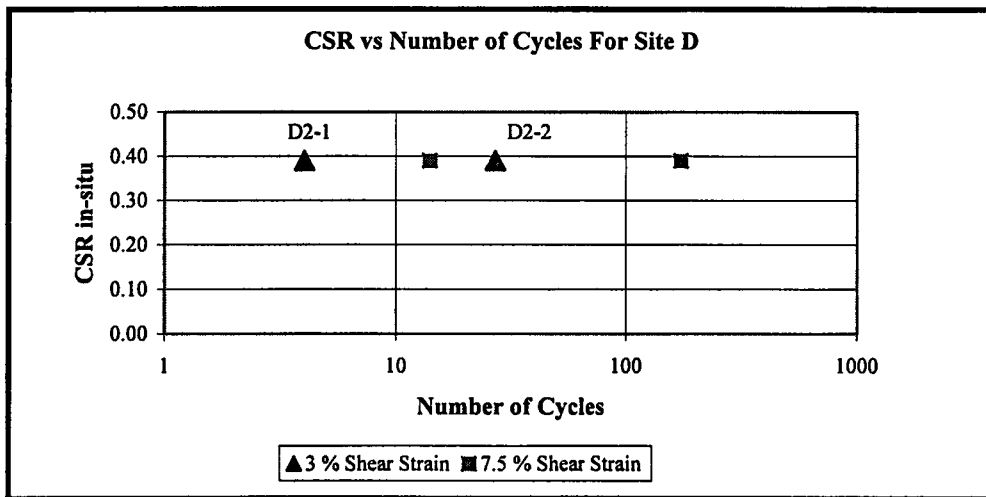


Figure 4.10 CSR vs. Number of Cycles For Site D

4.2.4 Site E

Two tests were performed on the samples retrieved from depths of 4.68 m (E1-2) and 4.79 m (E1-3) with the engineering properties as summarized in Table 4-5, Figure 4.11, Table 4-6 and Figure 4.13, respectively. Both samples were defined as fat clays with $PI > 32$.

As shown in Figure 4.12, the sample of E1-2, as a result of applied deviatoric load expressed in terms of a $CSR_{in-situ}$ of 0.47, can be concluded as liquefied after 20 cycles both 100% pore pressure ratio-based or 5% double amplitude axial strain definitions of liquefaction is used. The rapid pore pressure generation behaviour is very similar to what we have observed with silt and sands. Once again as these test results have shown, clays can liquefy (both in the sense of pore pressure generation and threshold strain) under cyclic loads if enough cycles are produced.

Figure 4.14 presents the results of cyclic triaxial tests performed on sample E1-3. As it is clearly seen on “number of cycles versus excess pore pressure ratio”

Table 4-5 Engineering Properties of Specimen E1-2

Borehole ID	SPT-E1	Sample ID	E1-4 / UD-1
Specimen ID	E1-2	Depth of Specimen (m)	4.68 (4.65-4.72)
Depth to Water Table (m)	0.7	Liquid Limit (%)	61
G_s	2.74	Plastic Limit (%)	28
Water Content (%)	39	Plasticity Index (PI)	32
Fines Content - <0.074mm (%)	95	Clay Content - <0.002mm (%)	33
C_u	>6	C_c	~1
Initial Void Ratio	1.02	Final Void Ratio	0.94
B Value		0.95	
Unified Soil Class.		Fat Clay (CH)	

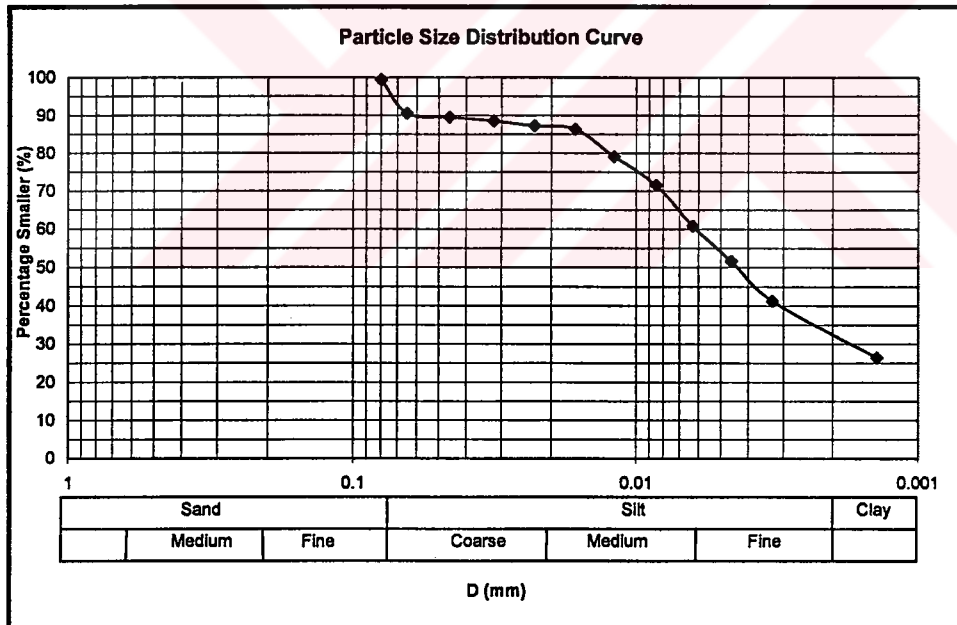


Figure 4.11 Particle Size Distribution for Specimen E1-2

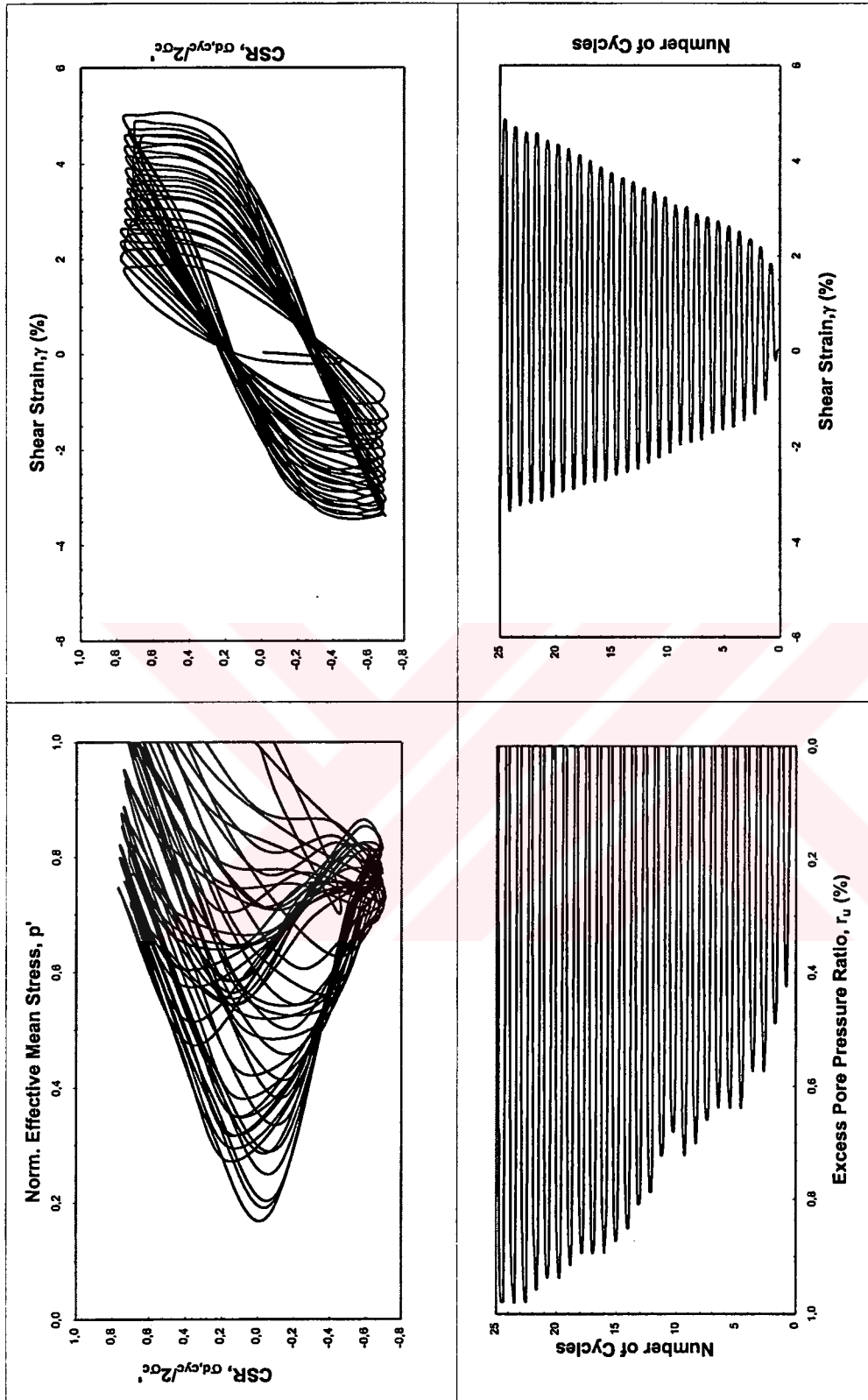


Figure 4.12 CTX Results for Specimen E1-2

Table 4-6 Engineering Properties of Specimen E1-3

Borehole ID	SPT-E1	Sample ID	E1-4 / UD-1
Specimen ID	E1-3	Depth of Specimen (m)	4.79 (4.75-4.82)
Depth to Water Table (m)	0.7	Liquid Limit (%)	62
G_s	2.67	Plastic Limit (%)	27
Water Content (%)	32	Plasticity Index (PI)	35
Fines Content - <0.074mm (%)	96	Clay Content - <0.002mm (%)	37
C_u	>5	C_c	<1
Initial Void Ratio	1.02	Final Void Ratio	N/A
B Value		0.96	
Unified Soil Class.		Fat Clay (CH)	

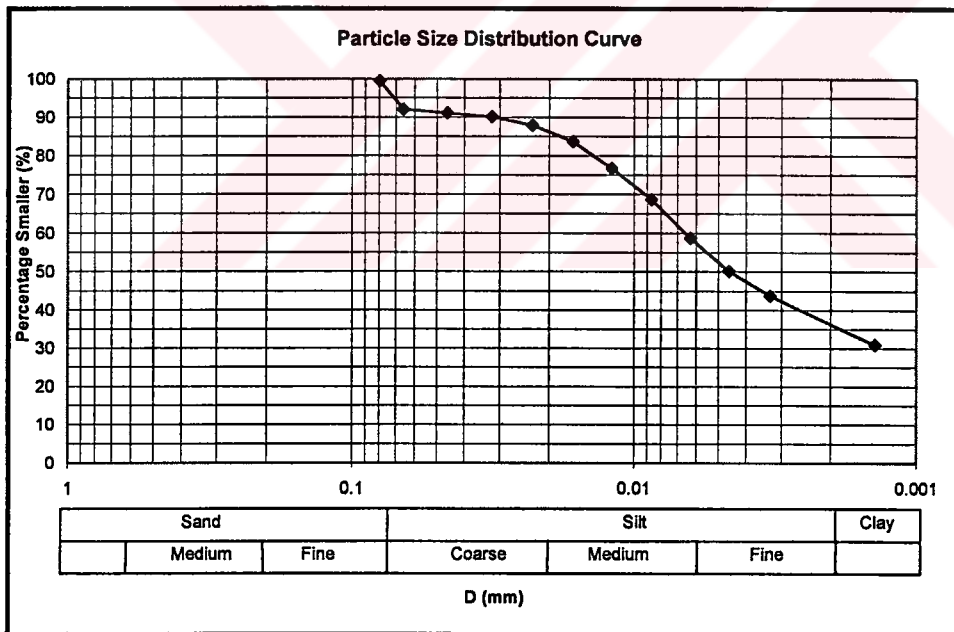


Figure 4.13 Particle Size Distribution for Specimen E1-3

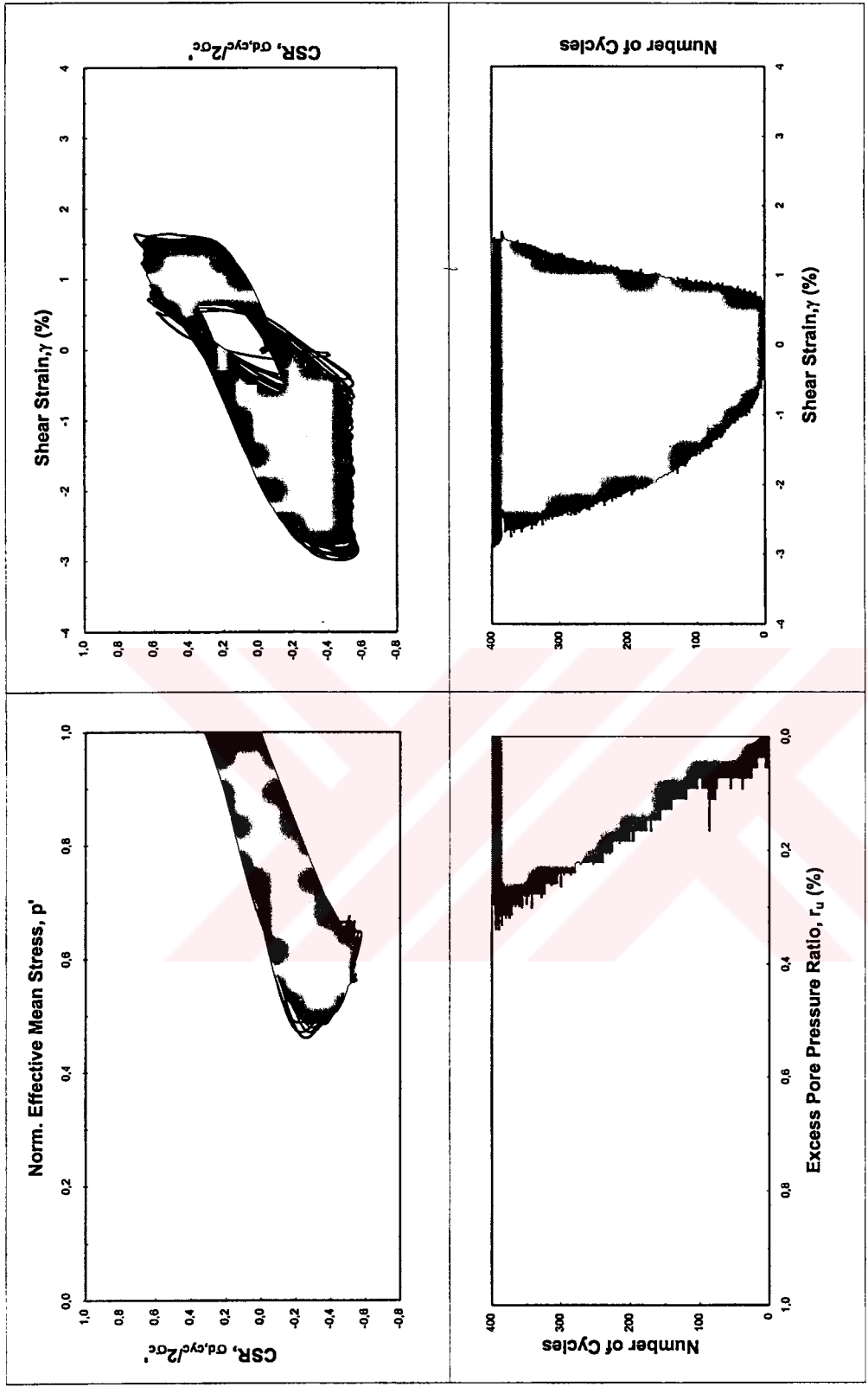


Figure 4.14 CTX Results for Specimen E1-3

plot, sample gradually develops pore pressure at applied CSR of 0.38. However it did accumulate neither enough pore pressure nor enough strains leading to the conclusion that sample has not liquefied.

Figure 4.15 summarizes the results of cyclic triaxial tests performed on samples acquired from site E. Both, 3% and 7.5% shear strain based CSR versus number of cycles plots are shown. The main difference in the behaviour of two samples with identical engineering properties is in the deviatoric loads applied.

Sample E1-2 liquefied at a CSR of 0.47 however sample E1-3 did not liquefy at a CSR of 0.38. It is interesting to observe the dramatic change in behaviour with minor changes in CSR.

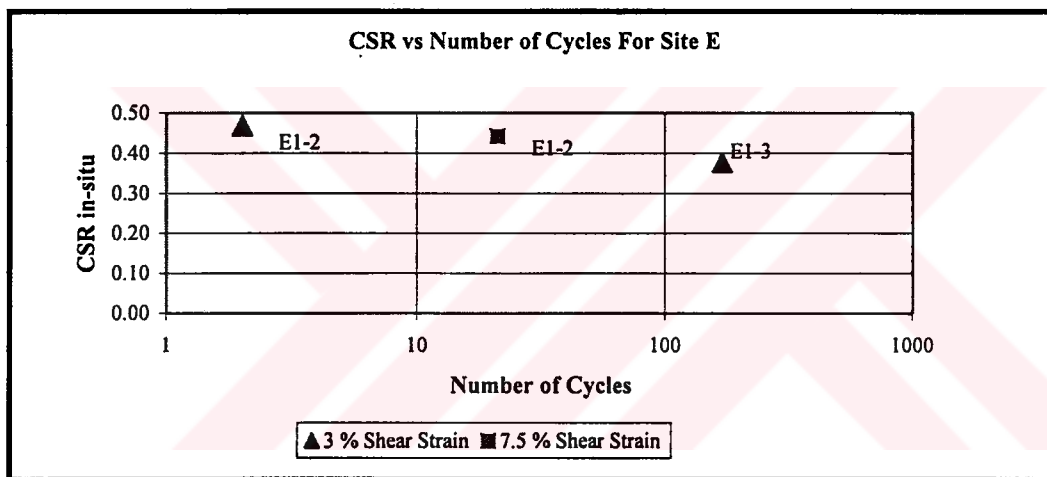


Figure 4.15 CSR vs. Number of Cycles For Site E

4.2.5 Site G

Two tests were performed on the samples retrieved from depths of 3.49 m (G2-1) and 4.05 m (G2-5) with the engineering properties as summarized in Table

Table 4-7 Engineering Properties of Specimen G2-1

Borehole ID	SPT-G2	Sample ID	G2-3 / UD-1
Specimen ID	G2-1	Depth of Specimen (m)	3.49 (3.45-3.53)
Depth to Water Table (m)	0.4	Liquid Limit (%)	35
G_s	2.66	Plastic Limit (%)	26
Water Content (%)	38	Plasticity Index (PI)	8
Fines Content - <0.074mm (%)	90	Clay Content - <0.002mm (%)	10
C_u	16.00	C_c	1.9
Initial Void Ratio	0.86	Final Void Ratio	0.69
B Value		0.95	
Unified Soil Class.		Silt (ML)	

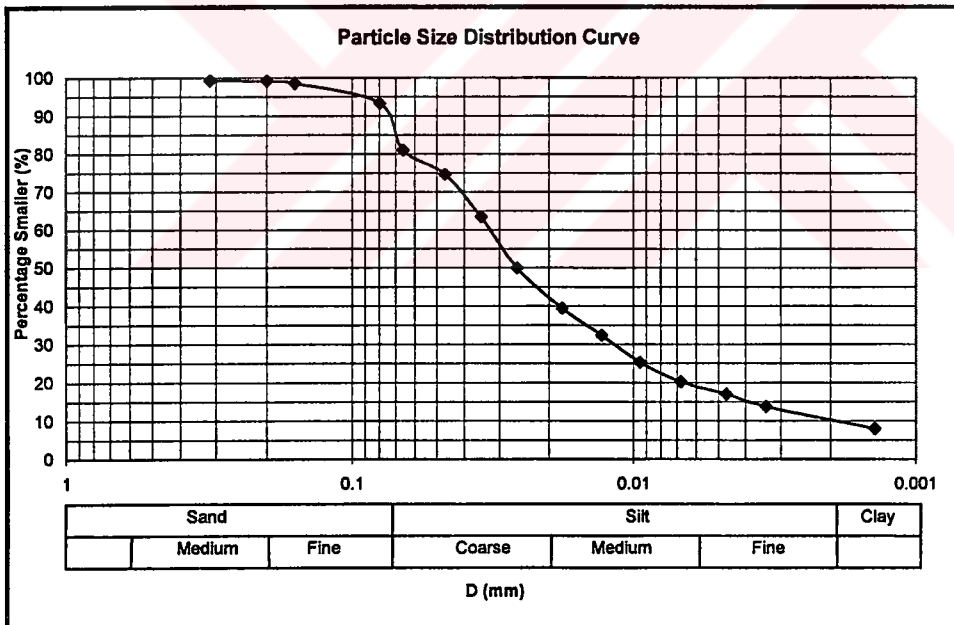


Figure 4.16 Particle Size Distribution for Specimen G2-1

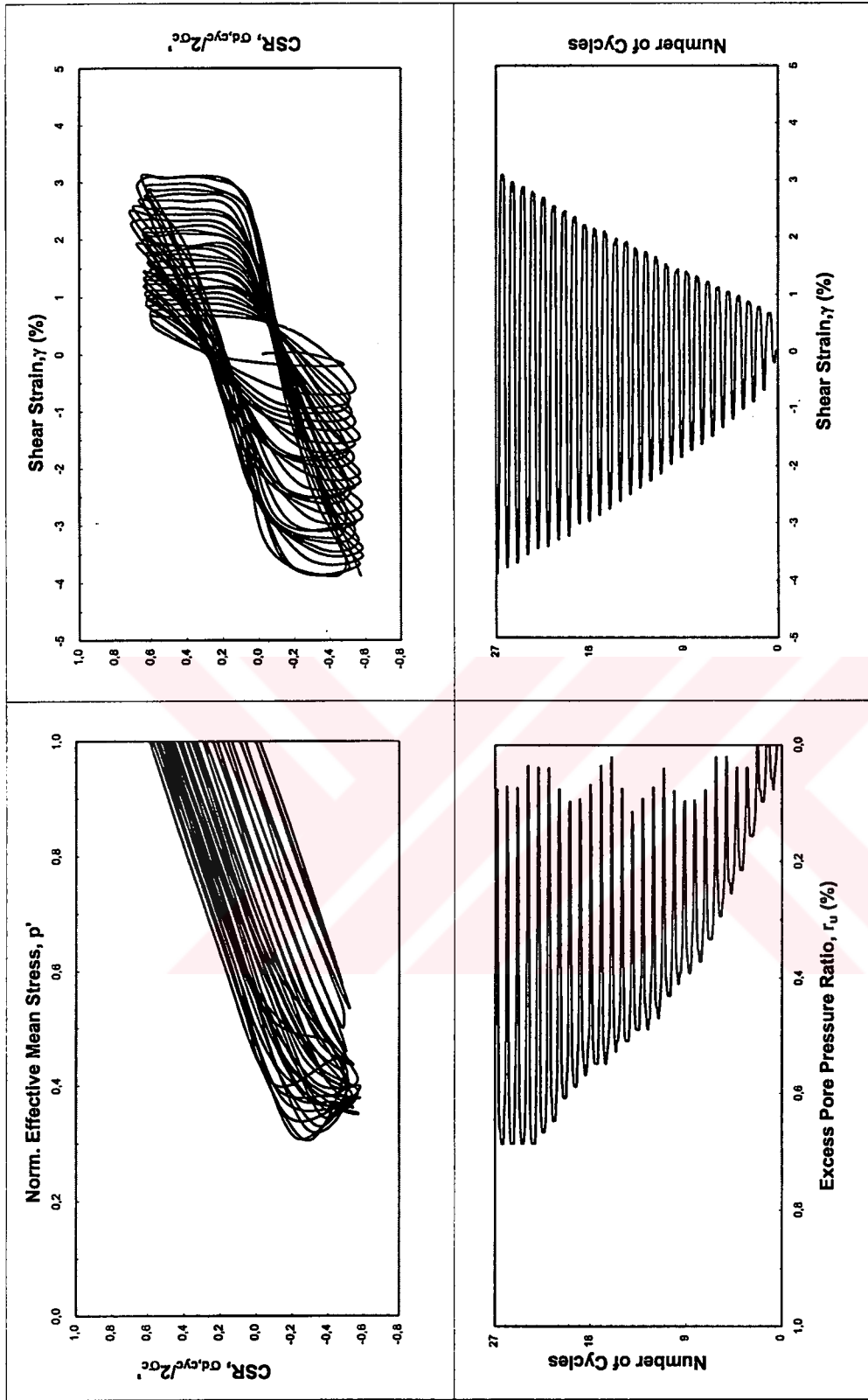


Figure 4.17 CTX Results for Specimen G2-1

Table 4-8 Engineering Properties of Specimen G2-5

Borehole ID	SPT-G2	Sample ID	G2-3 / UD-1
Specimen ID	G2-5	Depth of Specimen (m)	4.05 (4.01-4.08)
Depth to Water Table (m)	0.4	Liquid Limit (%)	58
G_s	2.67	Plastic Limit (%)	29
Water Content (%)	49	Plasticity Index (PI)	30
Fines Content - <0.074mm (%)	95	Clay Content - <0.002mm (%)	40
C_u	>5	C_c	>1
Initial Void Ratio	1.14	Final Void Ratio	0.86
B Value		0.95	
Unified Soil Class.		Fat Clay (CH)	

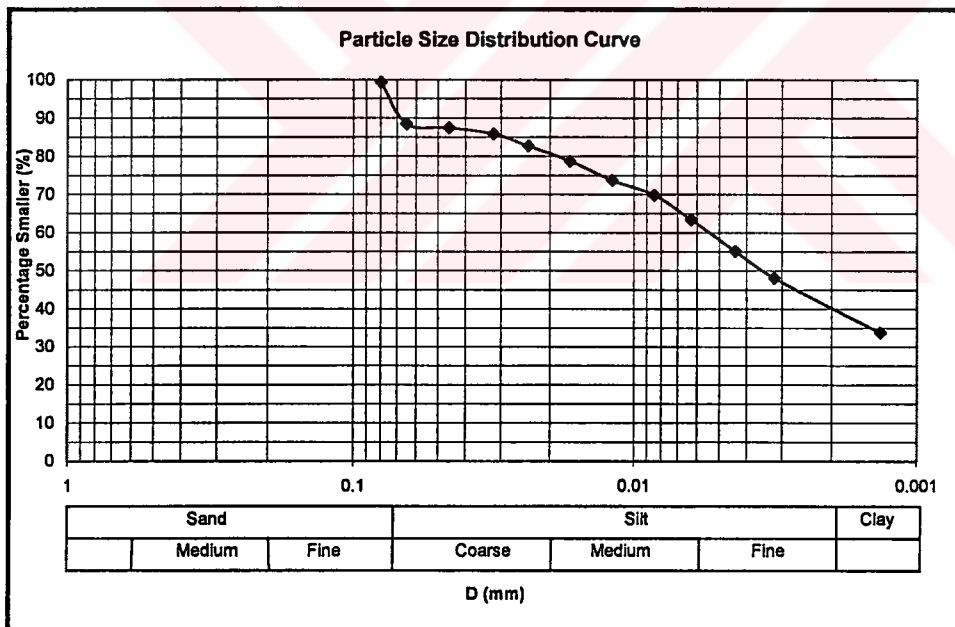


Figure 4.18 Particle Size Distribution for Specimen G2-5

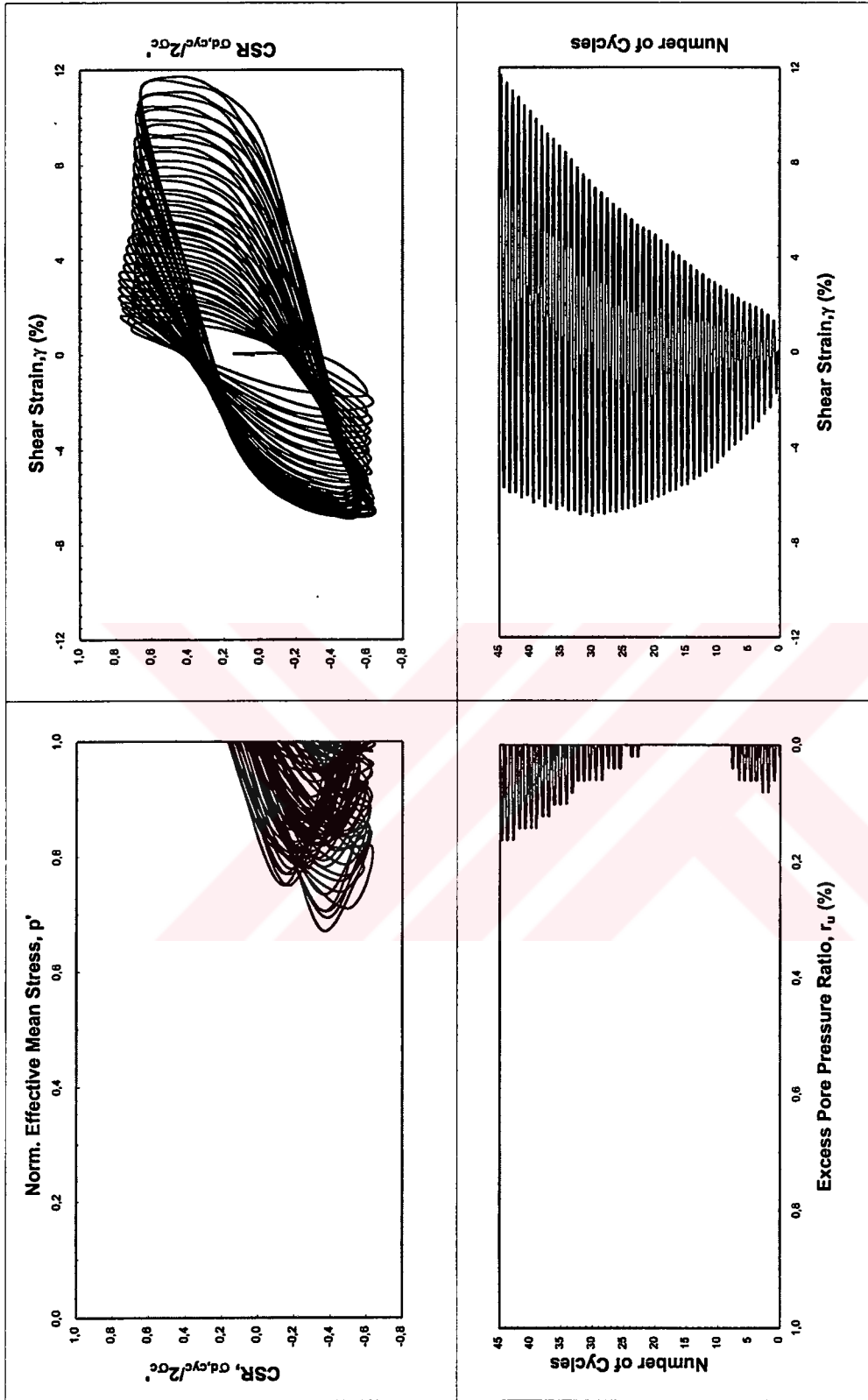


Figure 4.19 CTX Results for Specimen G2-5

4-7, Figure 4.16, Table 4-8 and Figure 4.18, respectively. Sample G2-1 is defined as silt with PI of ~8 and sample G2-5 is defined as fat clay with PI of 30.

As shown in Figure 4.17, the sample of G2-1, as a result of applied deviatoric load expressed in terms of a $CSR_{in-situ}$ of 0.39, can be concluded as non-liquefied after 27 cycles if 100% pore pressure ratio-based liquefaction definition is adopted. However, after 27 cycles 5% double amplitude axial strain is well developed. Rapid pore pressure generation behaviour is not surprising since the sample G2-1 is defined as silt (ML) with clay content of 10% and PI, 8%.

Figure 4.18 presents the results of cyclic triaxial tests performed on sample G2-5. As it is clearly seen on “number of cycles versus excess pore pressure ratio” plot, sample does not develop significant pore pressure as a result of applied CSR of 0.45. As opposed to the other fat clay samples, the sample did not liquefy at selected deviatoric load. A possible reason for this could be high PI of the sample (PI=30) compared to those that liquefied with a PI of 10%.

Figure 4.20 summarizes the results of cyclic triaxial performed on samples acquired from site G. Both 3% and 7.5% shear strain based CSR versus number of cycles plots are shown. As can be clearly seen from this figure that as a result of similar shaking intensity and duration to the ones recorded in Adapazarı after İzmit earthquake, foundation soils can easily accumulate 3-4% shear strain (corresponding to 1.5-2% axial strain).

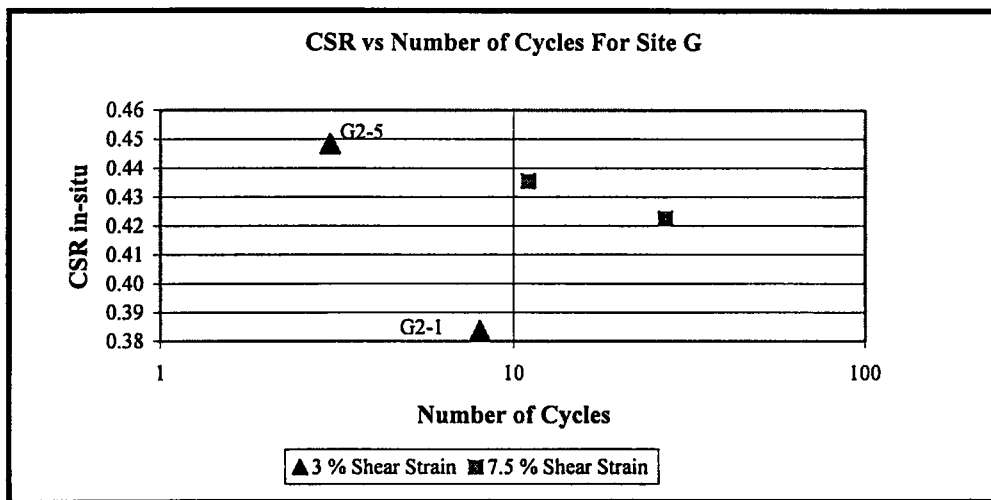


Figure 4.20 CSR vs. Number of Cycles For Site G

4.2.6 Site J

Three tests were performed on the samples retrieved from depths of 2.37 m (J3-1), 2.47 m (J3-2) and 2.57 m (J3-3) with the engineering properties as summarised in Table 4-9, Figure 4.21, Table 4-10, Figure 4.23, Table 4-11, Figure 4.25, respectively. All of the samples were defined as non-plastic samples (ML) except sample J3-2 which was defined as plastic silt with PI of 6%.

As shown in Figure 4.22, the sample of J3-1, as a result of applied deviatoric load expressed in terms of a $CSR_{in-situ}$ of 0.39, can be concluded as liquefied after 60 cycles if 100% pore pressure ratio-based liquefaction definition is adopted. However, after 24 cycles, 5% double amplitude axial strain is well developed. The gradual pore pressure generation behaviour is very similar to the ones observed in sands.

Figure 4.24 presents the results of cyclic triaxial tests performed on sample J3-2. As it is clearly seen on “number of cycles versus excess pore pressure ratio” plot, sample does not develop 100% pressure after over 100 cycles at an applied

Table 4-9 Engineering Properties of Specimen J3-1

Borehole ID	SPT-J3	Sample ID	J3-1 / UD-1
Specimen ID	J3-1	Depth of Specimen (m)	2.37 (2.33-2.40)
Depth to Water Table (m)	2.3	Liquid Limit (%)	Non Plastic
G_s	2.68	Plastic Limit (%)	Non Plastic
Water Content (%)	32	Plasticity Index (PI)	N/A
Fines Content - <0.074mm (%)	85	Clay Content - <0.002mm (%)	8
C_u	12.9	C_c	2.4
Initial Void Ratio	0.93	Final Void Ratio	0.83
B Value		0.96	
Unified Soil Class.		Silt with Sand (ML)	

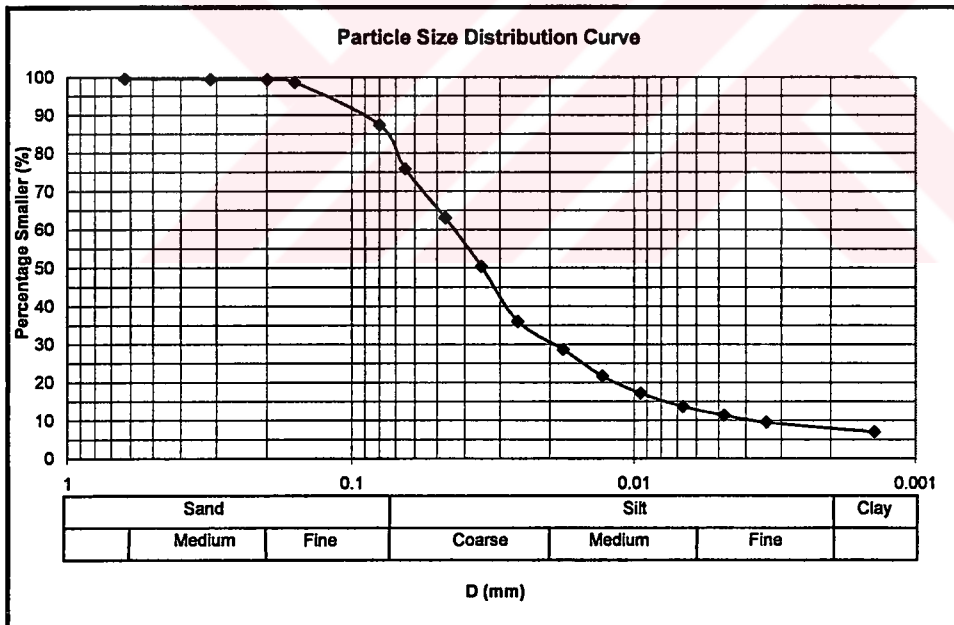


Figure 4.21 Particle Size Distribution for Specimen J3-1

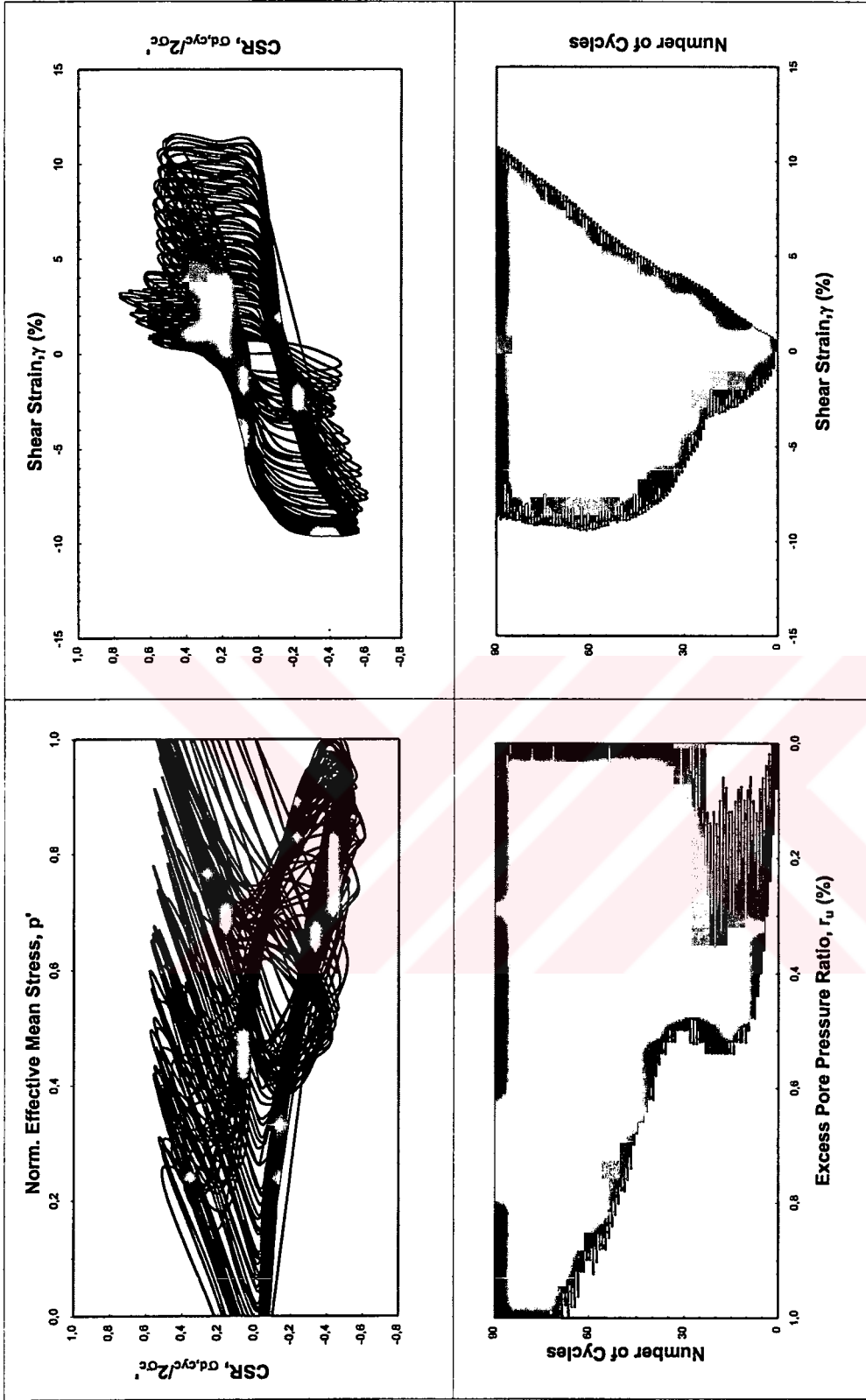


Figure 4.22 CTX Results for Specimen J3-1

Table 4-10 Engineering Properties of Specimen J3-2

Borehole ID	SPT-J3	Sample ID	J3-1 / UD-1
Specimen ID	J3-2	Depth of Specimen (m)	2.47 (2.43-2.50)
Depth to Water Table (m)	2.3	Liquid Limit (%)	30
G_s	2.65	Plastic Limit (%)	25
Water Content (%)	30	Plasticity Index (PI)	6
Fines Content - <0.074mm (%)	83	Clay Content - <0.002mm (%)	10
C_u	21.0	C_c	3.0
Initial Void Ratio	0.77	Final Void Ratio	0.70
B Value		0.95	
Unified Soil Class.		Silt (ML)	

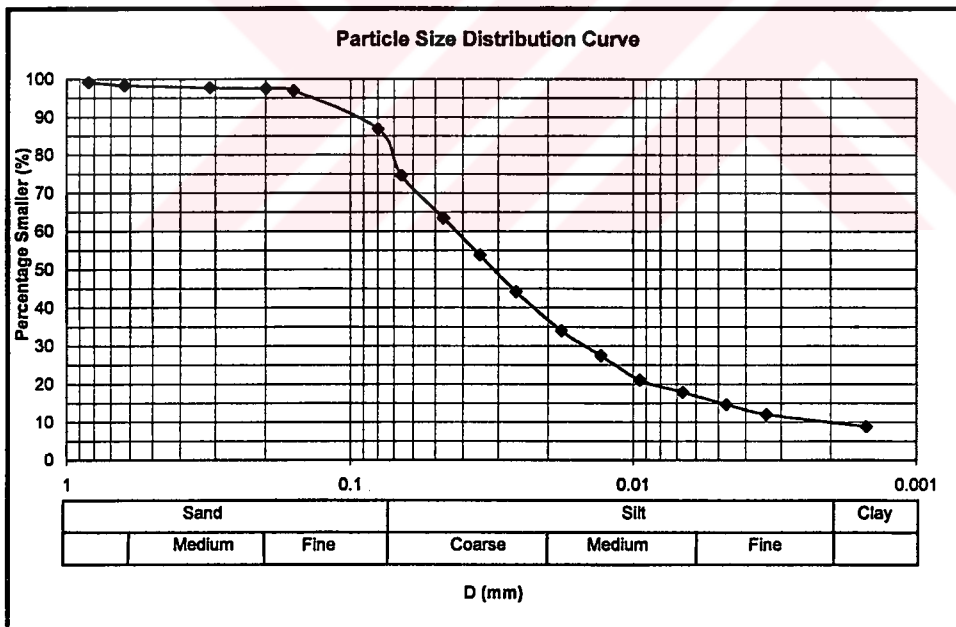


Figure 4.23 Particle Size Distribution for Specimen J3-2

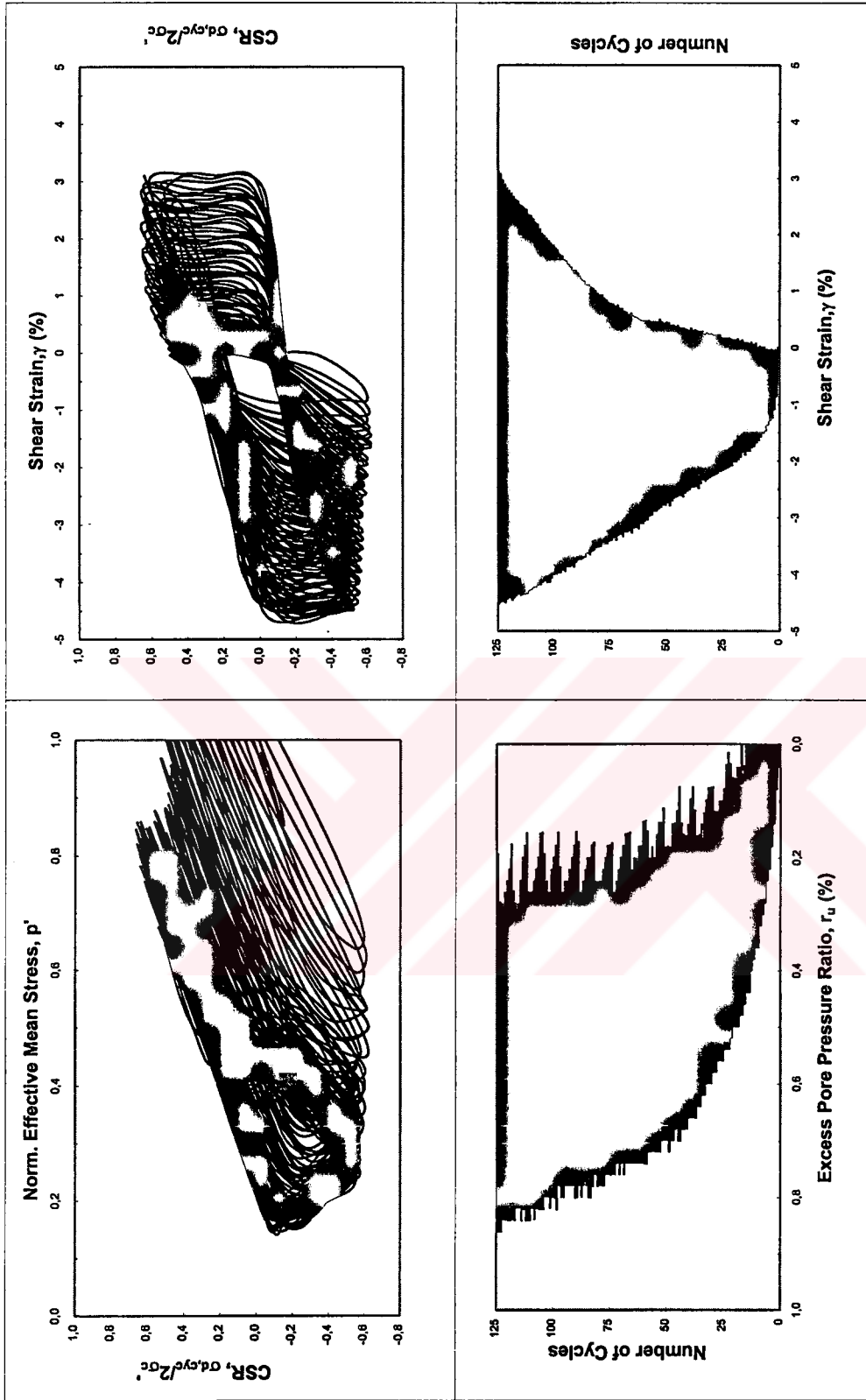


Figure 4.24 CTX Results for Specimen J3-2

Table 4-11 Engineering Properties of Specimen J3-3

Borehole ID	SPT-J3	Sample ID	J3-1 / UD-1
Specimen ID	J3-3	Depth of Specimen (m)	2.57 (2.53-3.60)
Depth to Water Table (m)	2.3	Liquid Limit (%)	Non Plastic
G_s	2.64	Plastic Limit (%)	Non Plastic
Water Content (%)	29	Plasticity Index (PI)	N/A
Fines Content - <0.074mm (%)	48	Clay Content - <0.002mm (%)	8
C_u	19.25	C_c	4.0
Initial Void Ratio	0.84	Final Void Ratio	0.71
B Value		0.95	
Unified Soil Class.		Sandy Silt (ML)	

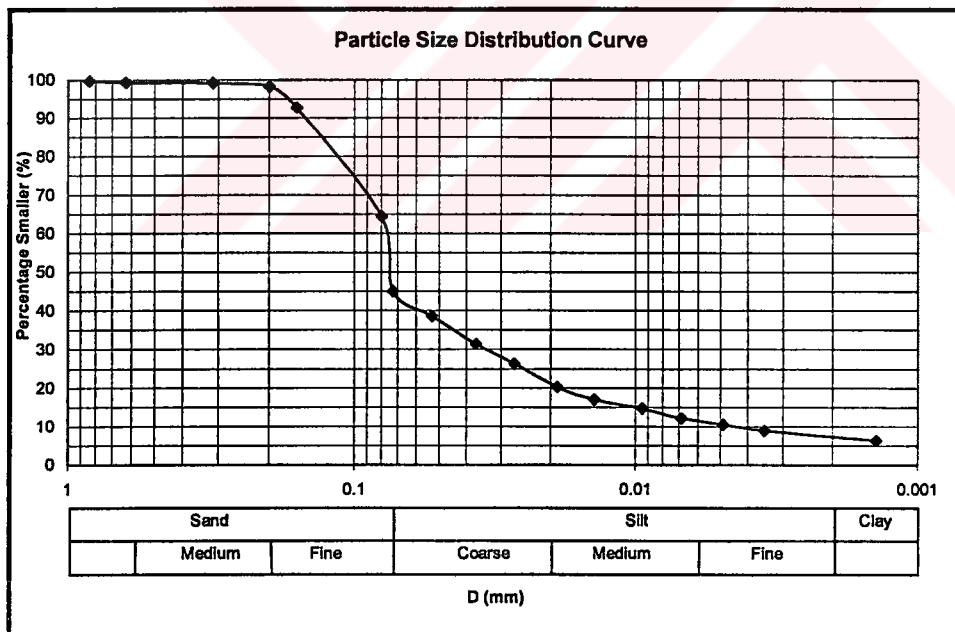


Figure 4.25 Particle Size Distribution for Specimen J3-3

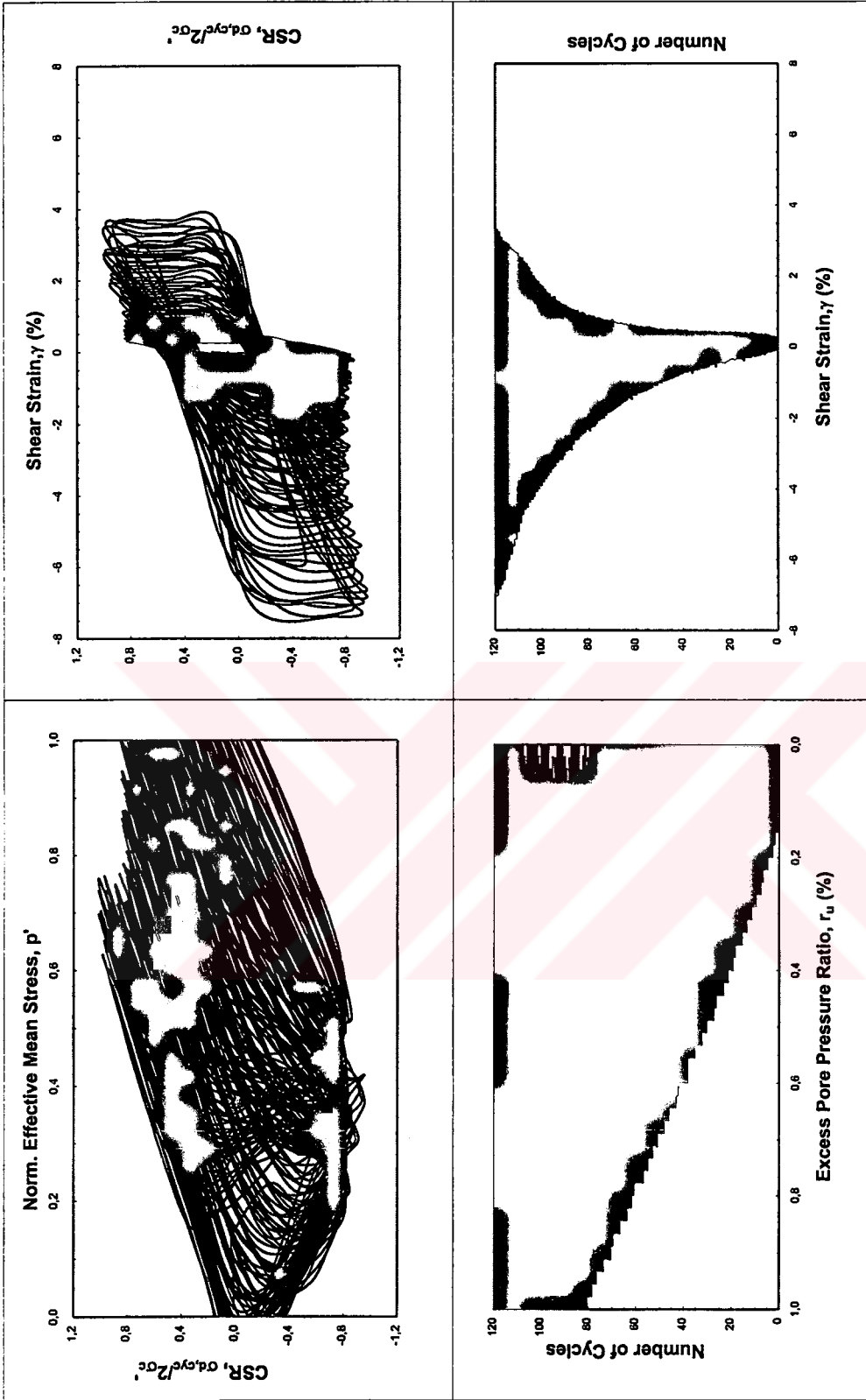


Figure 4.26 CTX Results for Specimen J3-3

CSR of 0.31. However at 124th cycle sample reached to a 5% double amplitude axial strain.

Figure 4.26 presents the results of cyclic triaxial tests performed on sample J3-3. As it is clearly seen on “number of cycles vs. excess pore pressure ratio” plot, sample develops 100% pore pressure after over 80th cycle of applied CSR of 0.52. Similarly 5% double amplitude axial strain is reached at 109th cycle.

Figure 4.27 summarizes the results of cyclic triaxial performed on samples acquired from site J. Both 3% and 7.5% shear strain based CSR vs. Number of cycles plots are shown. Since sample J3-2 is tested under relatively smaller deviatoric loads and PI of this sample is significantly higher than the other two, pore pressure generation and strain accumulation of it is relatively slower. (As can be clearly seen from Figure 4.27 that as a result of similar shaking intensity and duration to the ones recorded in Adapazarı after İzmit earthquake, foundation soils can easily accumulate 7.5% shear strain, corresponding to 5% axial strain.

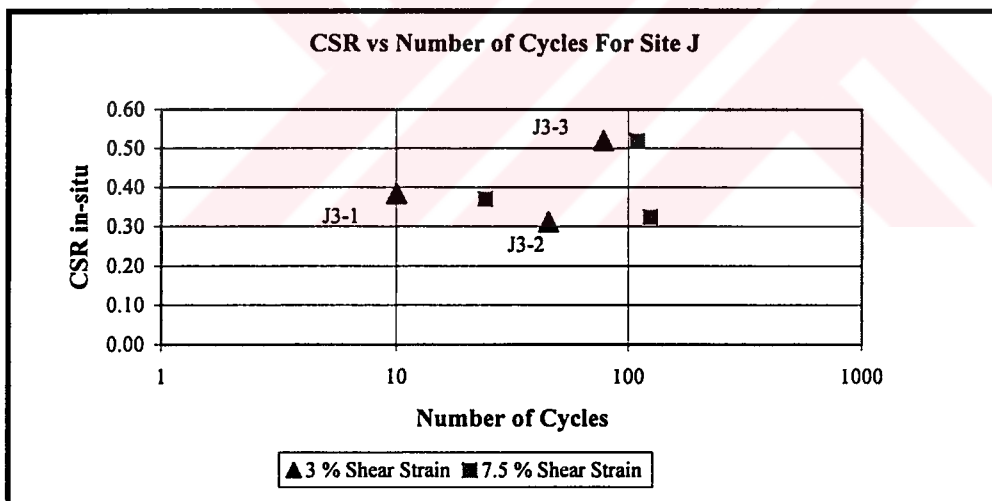


Figure 4.27 CSR vs. Number of Cycles For Site J

CHAPTER 5

SUMMARY AND CONCLUSION

5.1 SUMMARY

The purpose of this study was to develop a sound understanding of the behaviour of Adapazarı clayey silt and silty clays. For this purpose, series of cyclic triaxial tests were performed on 5 selected significant foundation displacement sites. These tests were performed by Geonor made, Norwegian cyclic triaxial testing apparatus. Samples were isotropically consolidated to building foundation effective stresses varying in the range of 0.45 to 0.55 atm. Volumetric strains were recorded during consolidation. Cyclic loads were chosen similar to the ones that were estimated in Adapazarı after İzmit earthquake in the range of CSR of 0.3 to 0.55 and applied with a frequency of 1 Hz. After the end of cyclic loading, samples were re-consolidated back to its initial effective consolidation stresses and the volumetric strains due to reconsolidation were once again recorded. Table 5-1 summarizes the engineering properties as well as the cyclic triaxial test results of tested soils.

As discussed in Chapter 4, the result of these cyclic triaxial tests were presented in the form of four scaled plots, which are:

- i. Normalized effective mean stress versus cyclic stress ratio (CSR)
- ii. Number of cycles versus excess pore pressure ratio
- iii. Shear strain versus CSR
- iv. Shear strain versus number of cycles

Table 5-1 Summary of the engineering properties and CSR values for all specimens

Specimen ID	Liquid Limit	Plastic Limit	Plasticity Index	Water Content (%)	Clay Content (%)	Fines Content (%)	$e_{initial}$	e_{final}	CSR _x	Number of Cycles	
										$\gamma=3\%$	$\gamma=7.5\%$
C1-1	58	23	35	39	37	97	1.01	0.95	0.56	155	910
C1-3	34	25	9	36	23	93	0.94	0.89	0.90	6	27
D2-1	30	23	7	32	15	72	0.86	0.78	0.60	4	14
D2-2	31	22	8	29	10	83	0.75	0.69	0.60	27	173
E1-2	61	28	32	39	33	95	1.02	0.94	0.70	2	21
E1-3	62	27	35	32	37	96	1.02	N/A	0.58	170	N/A
G2-1	35	26	8	38	10	90	0.86	0.69	0.63	8	27
G2-5	58	29	30	49	40	95	1.14	0.86	0.68	3	11
J3-1	N/P	N/P	N/P	32	8	85	0.93	0.83	0.58	10	24
J3-2	30	25	6	30	10	83	0.70	0.70	0.49	45	124
J3-3	N/P	N/P	N/P	29	8	48	0.84	0.71	0.80	78	109

These four scaled plots enable to clearly observe the change in;

- i. Stiffness
- ii. Effective Stress
- iii. Strain as a result of deviatoric load
- iv. Strain as a result of number of cycles

In addition to four scaled plots per each cyclic test, also for each site a “CSR versus Number of cycles” plot were also presented. These plots are drawn according to both 3% and 7.5% shear strain criteria. These plots will be the ideal tools for deciding if recorded shaking in Adapazari after 1999 is strong enough to trigger liquefaction. However, due to scarcity of cyclic test results on silty clays and clayey silts in the literature, comparisons of cyclic behaviour of similar soils from the literature were not possible.

5.2 CONCLUSION

The results of cyclic triaxial tests performed on selected Adapazari silty clays to clayey silts were judged to present a clear explanation of ground failure induced damage in Adapazari. Following conclusions could be drawn from presented cyclic triaxial test results:

1. Mixtures of silt and clays can be cyclically liquefied based on both 100% pore pressure or 5% double amplitude axial strain definitions. Current classification of liquefiable soils based on Modified Chinese criteria (Andrews and Martin, 2000) does not successfully identify liquefaction triggering risk as shown in Figure 5.1.

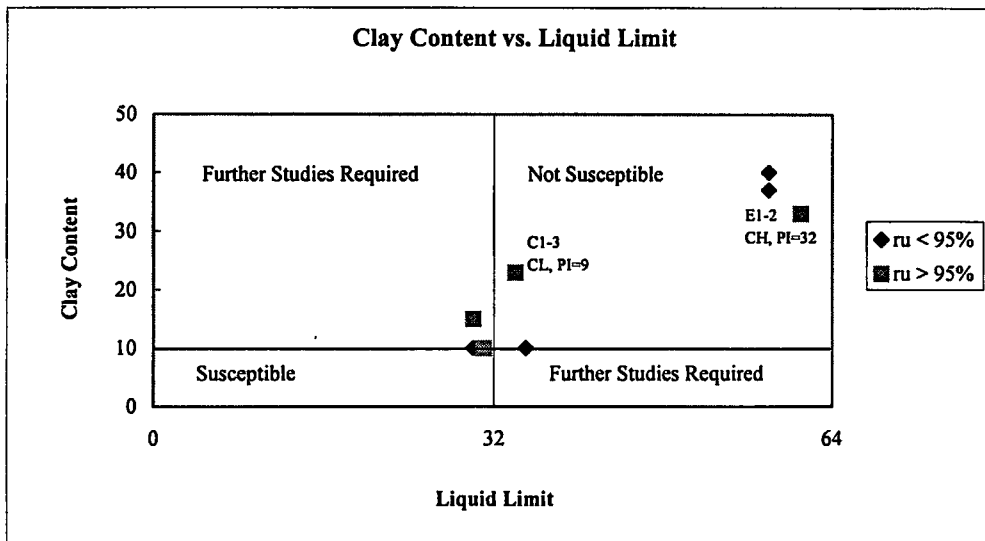


Figure 5.1 Liquefaction Susceptibility of Silty and Clayey Sands (after Andrews and Martin, 2000) and the findings of this study

2. Pore pressure built-up in silty clays and clayey silts are generally slower than the ones observed in sands and non-plastic silts. However low to medium plasticity silty clays and clayey silts can build up significant pore pressures ($r_u > 70\%$) under reasonably low number of cyclic loads ($N < 25$) at moderate to high CSR's (0.35 to 0.5).
3. Cyclic resistance of the mixtures of clays and silts increase with decrease in void ratio and increase in PI.
4. As shown in Figures 5.2 and 5.3, represented by the shaded region under 15 to 20 cycles of loads expressed in terms of CSR in the range of 0.4 to 0.5, similar to the values estimated in Adapazari after 1999, İzmit earthquakes (Bakır et. al., 2002). Adapazari silty clay and clayey silt mixtures can be cyclically mobilized or liquefied producing shear strains in the range of 3 to 7.5%. These high levels of shear strains can,

by themselves, explain the most of the foundation displacements observed in Adapazari.

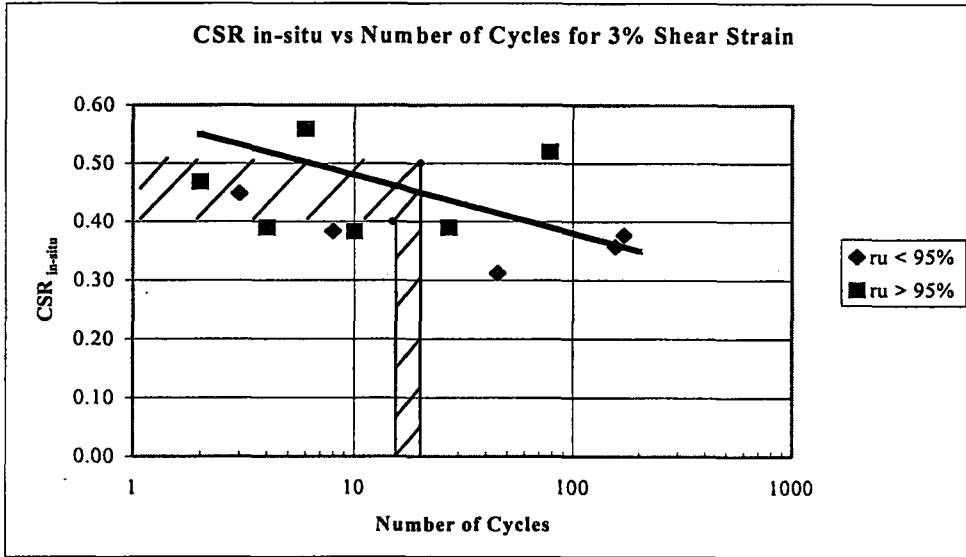


Figure 5.2 CSR_{in-situ} vs. Number of cycles for 3% Shear Strain

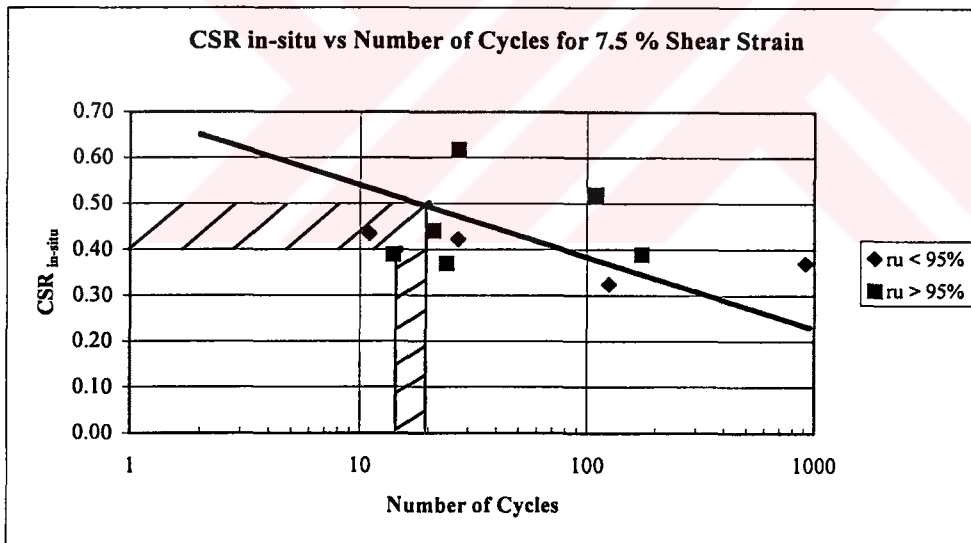


Figure 5.3 CSR_{in-situ} vs. Number of cycles for 7.5% Shear Strain

- Development of deviatorically and volumetrically based strain predictions as a function of some in-situ index test.
- Back analyses of foundation deformations observed in Adapazari by using the results of further studies recommended above.



REFERENCES

1. Ambraseys, N., Zapotek, A. (1969). "The Mudurnu Valley earthquake of July 22nd 1967", Bulletin of Seismological Society of America, Vol. 59, No. 2, pp. 521-589.
2. Andrews, D. C. A., Martin, G. R. (2000). "Criteria for Liquefaction of Silty Soils", Twelveth World Conference on Earthquake Engineering , Proceedings, Auckland, New Zeland.
3. Annaki, M., Lee K. L. (1977). "Equivalent Uniform Number of Cycle Concept for Soil Dynamics", Journal of Geotechnical Engineering Division, ASCE, Vol. 103, No. GT6, pp. 549-564.
4. Bakır, S., Sucuoğlu, H., Yılmaz, T. "An Overview of Local Site Effects and the Associated Building Damage in Adapazarı During the 17 August 1999, İzmit Earthquake" (Accepted for publication by Bulletin of Seismological Society of America, in 2001)
5. Boulanger, R. W., Seed, R. B. (1995). "Liquefaction of Sand Under Bidirectional Monotonic and Cyclic Loading", Journal of Geotechnical Engineering, ASCE, Vol. 121, No. GT12, pp. 870-878.
6. Castro, G. (1975). "Liquefaction and Cyclic Mobility of Sands", Journal of Geotechnical Engineering , ASCE, Vol. 101, No. GT6, pp. 551-569.
7. Castro, G., Poulos, S. J. (1976). "Factors Affecting Liquefaction and Cyclic Mobility", Proceedings of Symposium on Soil Liquefaction, ASCE National Convention, Philadelphia, October 1, 1976.

8. Chan, C. K. (1981). "An electropneumatic Cyclic Loading System", *Geotechnical Testing Journal*, ASTM, Vol. 4., No. 4, pp. 183-187.
9. Erdik, M. (2001). "Report on Kocaeli and Düzce (Turkey) Earthquakes", Boğaziçi University Kandilli Observatory & Earthquake Research Institute, Earthquake Engineering Department Report, İstanbul.
10. *Earthquake Spectra*, Chapter 8, (2000). Supplement A to Volume 16, 1999 Kocaeli, Turkey, Earthquake Reconnaissance Report.
11. Finn, W. D. L., and Bransby, P. L. and Pickering, D. J. (1970). "Effect of Strain History on Liquefaction of Sands", *Journal of the Soil Mechanics And Foundations Division*, ASCE, Vol. 93, No. SM6, pp. 1917-1934.
12. Kishida, H. (1966). "Damage to Reinforced Concrete Buildings in Niigata City with Special Reference to Foundation Engineering", *Soils and Foundations*, Vol. VII, No. 1.
13. Koizumi, Y (1966). "Change in Density of Sand Subsoil caused by the Niigata Earthquake", *Soils and Foundations*, Vol. VIII, No. 2, pp. 38-44.
14. Lee, K. L., Seed, H. B. (1977). "Cyclic Stress Conditions Causing Liquefaction of Sand", *Journal of the Soil Mechanics And Foundations Division*, ASCE, Vol. 93, No. SM1, pp. 47-70.
15. Li, X. S., Chan, C. K., Shen, C. K. (1988). "An Automated Triaxial Testing System", *Advanced Triaxial Testing of Soils and Rocks*, ASTM STP977, Donaghe, R. T., R. C. Chaney and M. L. Silver, American Society of Testing and Materials, pp. 95-106.
16. Mogami, H., Kubo, T. (1953). "The Behavior of Soil During Vibration", *Proceedings of the Third International Conference on Soil Mechanics and Foundation Engineering*, Vol. 1, pp. 152-153.
17. Mohamad, R., Dobry, R. (1986). "Undrained Monotonic and Cyclic Triaxial Strength of Sand", *Journal of Geotechnical Engineering Division*, ASCE, Vol. 112, No. 10, pp.941-958.
18. Mori, K., Seed, H. B., Chan, C. K. (1978). "Influence of Sample Disturbance on Sand Response to Cyclic Loading", *Journal of Geotechnical Engineering Division*, ASCE, Vol. 104, No. GT3, pp.323-339.

19. National Research Council, (1985). "Liquefaction of Soils During Earthquakes", Committee on Earthquake Engineering, National Academy Press.
20. Ohsaki, Y. (1966). "Niigata Earthquakes, 1964, Building Damage and Soil Conditions", Soils and Foundations, Vol. 6, No. 2, pp. 14-37.
21. Polito, P. C., Martin, J. R. (2001). "Effects of Nonplastic Fines on the Liquefaction Resistance of Sands", Journal of Geotechnical and Geoenvironmental Engineering, ASCE, Vol. 127, No. GT5, pp. 408-415.
22. Pyke, R. M., Seed, H. B., Chan, C. K. (1975). "Settlement of Sands under Multi-directional Loading", Journal of Geotechnical Engineering Division, ASCE, Vol. 101, No. GT4, pp.379-398.
23. Rathje, E. M. and Stokoe II, K. H. (2001). "Kocaeli and Düzce Earthquakes – Strong Motion Stations Data From SASW Testing", Pacific Earthquake Research Center Lifelines Quarterly Progress Meeting, Summary Notes, 1p.
24. Ray, R.P., Woods, R.D. (1988). "Modulus and Damping due to Uniform and Variable Cyclic Loading", Journal of Geotechnical Engineering Division, ASCE, Vol. 114, No. 8, pp. 861-876.
25. Robertson, P. K., Fear, C. E. (1997), "Earthquake Geotechnical Engineering", Ishihara (editor), Balkema, Rotterdam, pp. 1253-1289.
26. Seed, H. B., Lee, K. L. (1966). "Liquefaction of Saturated Sands During Cyclic Loading", Journal of the Soil Mechanics And Foundations Division, ASCE, Vol. 92, No. SM6, pp. 105-134.
27. Seed, H. B., Peacock, K. L. (1971). "Test Procedures for Measuring Soil Liquefaction Characteristics", Journal of the Soil Mechanics and Foundations Division, ASCE, Vol. 97, No. SM8, pp. 1099-1119.
28. Seed, H. B. (1976), "Liquefaction Problems in Geotechnical Engineering", Proceedings of Symposium on Soil Liquefaction, ASCE National Convention, Philadelphia, October 1, 1976.
29. Silver, M. L. (1977). "Laboratory Triaxial Testing Procedures to Determine the Cyclic Strength of Soils", NUREG-0031, National Technical Information Service, Springfield, Va.

30. Terzaghi, K., Peck, R. B. (1948). "Soil Mechanics in Engineering Practice", John Wiley and Sons, Inc., 2nd Edition.
31. Tezcan, S. (1973). " Microtremor Studies in Adapazarı, Turkey" Preprints Fifth World Conference on Earthquake Engineering, International Association for Earthquake Engineering, Rome, Vol. 3, pp. 763-766.
32. Vucetic, M., Dobry, R. (1988). "Effect of Soil Plasticity on Cyclic Response", Journal of Geotechnical Engineering Division, ASCE, Vol. 117, No. 1, pp. 89-107.
33. Yarar, R., Tezcan, S. Durgunoglu, H. T. (1977). " Soil Amplification Effects in the Adapazarı, Turkey, earthquake of 1967", Proceedings, Sixth World Conference on Earthquake Engineering, Sarita Prakashan, Meerut, India, Vol. 3, pp. 2435-2440.
34. 17 Ağustos 1999 Gölcük- Arifiye (Kuzeydoğu Marmara) Depremleri Sonrası Sakarya İli ve Ona Bağlı Yerleşkeler İçin Yerleşim Alanları Araştırma Raporu, Türkiye Bilimsel ve Teknik Araştırmalar Kurumu Yer Deniz Atmosfer Bilimleri ve Çevre Araştırma Grubu, Orta Doğu Teknik Üniversitesi Mühendislik Fakültesi Jeoloji Mühendisliği Bölümü, Maden Tetkik ve Arama Genel Müdürlüğü Jeoloji Etütleri Dairesi, Kasım 1999, Ankara.